nature communications

Article

https://doi.org/10.1038/s41467-024-54140-1

Pharmacological targeting of casein kinase 1δ suppresses oncogenic NRAS-driven melanoma

Received: 10 October 2023

Accepted: 3 November 2024

Published online: 21 November 2024

Check for updates

Yalei Wen[1,2,3,9], Hui Wang[4,5,9], Xiao Yang[3,9], Yingjie Zhu[3,9], Mei Li[3], Xiuqing Ma[3], Lei Huang[3], Rui Wan[3], Caishi Zhang[3], Shengrong Li[3], Hongling Jia[6], Qin Guo[7], Xiaoyun Lu[3], Zhengqiu Li[3], Xiangchun Shen[2], Qiushi Zhang[1] ✉, Lu Si[8] ✉, Chengqian Yin[4,5] ✉ & Tongzheng Liu[1,2,3] ✉

Activating mutations in NRAS account for 15–20% of melanoma, yet effective anti-NRAS therapies are still lacking. In this study, we unveil the casein kinase 1δ (CK1δ) as an uncharacterized regulator of oncogenic NRAS mutations, specifically Q61R and Q61K, which are the most prevalent NRAS mutations in melanoma. The genetic ablation or pharmacological inhibition of CK1δ markedly destabilizes NRAS mutants and suppresses their oncogenic functions. Moreover, we identify USP46 as a bona fide deubiquitinase of NRAS mutants. Mechanistically, CK1δ directly phosphorylates USP46 and activates its deubiquitinase activity towards NRAS mutants, thus promoting oncogenic NRAS-driven melanocyte malignant transformation and melanoma progression in vitro and in vivo. Our findings underscore the significance of the CK1δ-USP46 axis in stabilizing oncogenic NRAS mutants and provide preclinical evidence that targeting this axis holds promise as a therapeutic strategy for human melanoma harboring NRAS mutations.

RAS proteins are membrane-associated small GTPases that switch between the active GTP-bound and inactive GDP-bound states. In response to growth factors and other stimuli, the active GTP-bound RAS interacts with effectors containing RAS binding domain (RBD) to activate various downstream signaling pathways, thereby regulating proliferation and other cellular processes[1]. In mammals, three closely related RAS isoforms, KRAS, NRAS and HRAS, are frequently mutated in approximately 30% of all human cancers[2]. Among these mutations, NRAS mutations are found in 15–20% of melanomas and are associated with worse clinical outcomes[3]. The majority of NRAS mutations in melanoma occur at glutamine 61(Q61), with frequent substitution by arginine (R)(40%) and lysine (K)(29%) or leucine (L)(12%). These mutations lock NRAS in an active state and lead to growth factor-independent proliferation of melanocytes and transformation to melanoma[4]. Thus, developing effective therapies targeting these oncogenic NRAS mutants is critical for the treatment of oncogenic

[1]Research Institute for Maternal and Child Health, The Affiliated Guangdong Second Provincial General Hospital, Postdoctoral Research Station of Traditional Chinese Medicine, School of Pharmacy, Jinan University, Guangzhou 510632, China. [2]The State Key Laboratory of Functions and Applications of Medicinal Plants, Guizhou Medical University, Guiyang 550014, China. [3]College of Pharmacy/International Cooperative Laboratory of Traditional Chinese Medicine Modernization and Innovative Drug Development of Ministry of Education (MOE) of China, Jinan University, Guangzhou 510632, China. [4]Institute of Cancer Research, Shenzhen Bay Laboratory, Shenzhen 518107, China. [5]Shenzhen Medical Academy of Research and Translation (SMART), Shenzhen 518107 Guangdong, China. [6]Department of Medical Biochemistry and Molecular Biology, School of Medicine, Jinan University, Guangzhou 510632, China. [7]Department of Pathology, Shanxi Provincial People's Hospital, Taiyuan 030012, China. [8]Key Laboratory of Carcinogenesis and Translational Research (Ministry of Education), Department of Melanoma and Sarcoma, Peking University Cancer Hospital and Research Institute, Beijing 100142, China. [9]These authors contributed equally: Yalei Wen, Hui Wang, Xiao Yang, Yingjie Zhu. ✉e-mail: zhangqsh@gd2h.org.cn; silu15_silu@126.com; yincq@szbl.ac.cn; liutongzheng@jnu.edu.cn

NRAS-driven melanoma. Despite the recent development of inhibitors targeting KRAS mutants such as G12C, G12S, and G12D[5–7], there remain significant challenges in developing targeted therapy for hotspot mutants of NRAS. This difficulty arises primarily from the absence of well-defined binding pockets and its high affinity for endogenous GTP. Therefore, strategies that target upstream regulators of NRAS activity or its downstream signaling pathways might be appealing for treating cancers driven by oncogenic NRAS mutations, including melanoma.

The serine-threonine casein kinase 1 (CK1) isoforms, CK1δ and CK1ε, are closely related and share a high degree of sequence homology. These isoforms were originally reported to regulate the circadian rhythms of eukaryotic cells by phosphorylating clock proteins[8,9]. Recently, CK1δ and CK1ε have been implicated in various neurological disorders. Additionally, the deregulation of CK1δ and CK1ε activity has been shown to disrupt key cellular processes such as cell cycle progression, cell proliferation, and protein translation, contribute to tumorigenesis and tumor progression[10–13]. However, the specific role of CK1δ and CK1ε in melanocyte transformation and melanoma progression remains largely unexplored.

In this work, we demonstrate that PF670462, a potent and selective inhibitor of CK1δ/ε[14], achieves over 80% inhibition of NRAS Q61R activity. Furthermore, we reveal that the CK1δ isoform, rather than CK1ε, is crucial in sustaining oncogenic NRAS mutants by regulating its stabilization. We also identify USP46 as a previously unidentified deubiquitinase of NRAS mutants. Mechanistically, CK1δ directly phosphorylates and activates USP46, thereby promoting oncogenic NRAS-driven melanocyte transformation and tumor progression. Overall, our findings provide preclinical evidence that targeting the CK1δ-USP46 axis may represent an effective therapeutic strategy for oncogenic NRAS-driven melanoma.

Results

CK1δ is a critical regulator of oncogenic NRAS mutants

The activation of NRAS signaling depends on its association with the common RBD of effectors, such as Raf and PI3K[15]. Disrupting the NRAS-RBD interaction could represent alternative therapeutic strategies in oncogenic NRAS -driven melanoma. To achieve this objective, we screened for small molecule compounds that regulate the activity of NRAS Q61R, the most prevalent *NRAS* mutation in melanoma. SK-MEL-103 cells expressing FLAG-tagged NRAS Q61R was generated and an in-house small molecule library was screened by using a modified active NRAS chemiluminescence assay as a readout (Fig. 1a). We found that several compounds caused more than 70% inhibition of NRAS Q61R activity, among which the inhibitory effect of PF670462 was the most significant (Fig. 1a). The decrease of the active fraction of the endogenous NRAS mutants by PF670462 was validated in SK-MEL-103 cells harboring NRAS Q61R and SK-MEL-30 cells harboring NRAS Q61K by the active-RAS pull-down assay (Fig. 1b). Since PF670462 was reported to inhibit both CK1δ and CK1ε[14], we next determined which CK1 isoform is critical to regulate NRAS mutant. As shown in Fig. 1c, d, the knockdown of CK1δ rather than CK1ε significantly reduced the active fraction of NRAS Q61R in SK-MEL-103 cells. Intriguingly, such inhibitory effects of targeting CK1δ might be due to the decreased protein level of NRAS mutants since the treatment of PF670462 significantly reduced the protein level of NRAS mutant in SK-MEL-103, SK-MEL-30 and SK-MEL-2 carrying NRAS Q61R/K (Fig. 1e, f and Supplementary Fig. 1a). Similar results were also observed when SK-MEL-103 cells were treated with two other CK1δ inhibitors D4476 and Casein kinase 1δ-In-8 (Supplementary Fig. 1b–e). Moreover, the depletion of CK1δ but not CK1ε dramatically decreased the protein level of NRAS in SK-MEL-103 and SK-MEL-30 cells (Fig. 1g and Supplementary Fig. 1f, g). Regarding high sequence homology between three *RAS* isoforms, the potential effect of CK1δ inhibition on KRAS mutant was also examined. As shown in Supplementary Fig. 1h–j, the treatment of PF670462 did not significantly affect the protein level of KRAS mutants in KRAS-mutant NSCLC (A549 harboring KRAS G12S and NCI-H358 harboring KRAS G12C), pancreatic cancer (AsPC-1 harboring KRAS G12D and SU.86.86 harboring KRAS G12D) and colorectal cancer (LoVo harboring KRAS G13D and HCT116 harboring KRAS G13D). Moreover, the protein level of NRAS WT was not significantly affected by the treatment of PF670462 in A375 and A2058, two melanoma cell lines harboring NRAS WT (Supplementary Fig. 1k). These results indicate targeting CK1δ specifically regulates the protein level of NRAS Q61R/K mutants rather than NRAS WT or KRAS mutants.

The underlying mechanism of CK1δ to regulate NRAS mutants was next investigated. We found that the depletion or inhibition of CK1δ did not affect the transcription of NRAS (Fig. 1h, i). In contrast, the proteasome inhibitor MG132 could rescue the decreased protein level of NRAS mutants caused by the depletion or pharmacological inhibition of CK1δ, indicating a proteasome-dependent mechanism of CK1δ in the regulation of NRAS mutants (Fig. 1j–m and Supplementary Fig. 1l, m). In addition, results of cycloheximide pulse-chase assay shown that NRAS protein was less stable in CK1δ-depleted SK-MEL-103 (Fig. 1n), which might be due to the increased ubiquitination level of NRAS Q61R (Supplementary Fig. 1n). We also found that the treatment of PF670462, D4476 and Casein Kinase 1δ-In-8 potently increased the ubiquitylation level of NRAS Q61R/K (Fig. 1o, p and Supplementary Fig. 1o–q), meanwhile such an effect of CK1δ inhibition on NRAS Q61L ubiquitination was weak (Supplementary Fig. 1r).

Based on these results, we next examined the effect of targeting CK1δ on oncogenic NRAS mutant-dependent malignant phenotypes. As shown in Fig. 2a–g and Supplementary Fig. 2a–d, the depletion or inhibition of CK1δ in SK-MEL-103 cells, SK-MEL-30 cells and SK-MEL-2 cells significantly decreased p-AKT and p-ERK levels, two known downstreams of RAS signaling, thereby inhibiting cellular proliferation, migration, and invasion abilities along with increased cellular sensitivity to dacarbazine (DTIC), one approved chemotherapeutic agent for metastatic melanoma[16]. In the line with these findings in vitro, similar results were observed in xenograft animal experiments, meanwhile the reconstitution of NRAS mutants largely rescued such phenotypic changes caused by the depletion or inhibition of CK1δ (Fig. 2h, i). Interestingly, the inhibition of CK1δ by PF670462 did not affect the sensitivity of *BARF*-mutated melanoma cells to DTIC (Supplementary Fig. 2e).

Previous reports shown that CK1α could phosphorylate β-catenin at Ser45, but did not affect the total level of β-catenin in several melanoma cell lines such as SK-MEL-19 and Sbcl2[17,18]. Negative regulators of Wnt/β-catenin signalings such as Axin were reported to increase the recruitment of β-TrCP to HRAS and promoted its degradation in colorectal cancer cell lines, while the over-expression of β-catenin blocked the recruitment of β-TrCP to HRAS and inhibited subsequent proteasome-dependent degradation of HRAS[19–21]. To figure out whether β-catenin is involved the regulation of NRAS mutant in melanoma cells, we next investigated the effect of CK1δ on β-catenin in SK-MEL-103 cells. As shown in Supplementary Fig. 2f, g, the depletion or inhibition of CK1δ by its pharmacological inhibitor Casein kinase 1δ-In-8 hardly affect both nuclear and cytosol levels of β-catenin in SK-MEL-103 cells. Moreover, the depletion and inhibition of β-catenin by its specific inhibitor MSAB at the concentration of 5 μM did not significantly decrease the protein level of NRAS Q61R mutant in SK-MEL-103 cells (Supplementary Fig. 2h, i). Together, these results indicate that the regulation of NRAS Q61R/K mutants by CK1δ is not β-catenin-dependent. The discrepancy with this previous report that the aberrant Wnt/β-catenin signaling regulates HRAS stability in colorectal cancer might be due to the various RAS isoforms and distinct cell-contexts.

Identification of the bona fide deubiquitinase of oncogenic NRAS mutants

CK1δ was reported to phosphorylate and regulate the degradation of its substrates such as Brg1[22]. To our surprise, the interaction between purified GST-CK1δ and His-NRAS Q61R was not detected (Fig. 3a),

https://doi.org/10.1038/s41467-024-54140-1

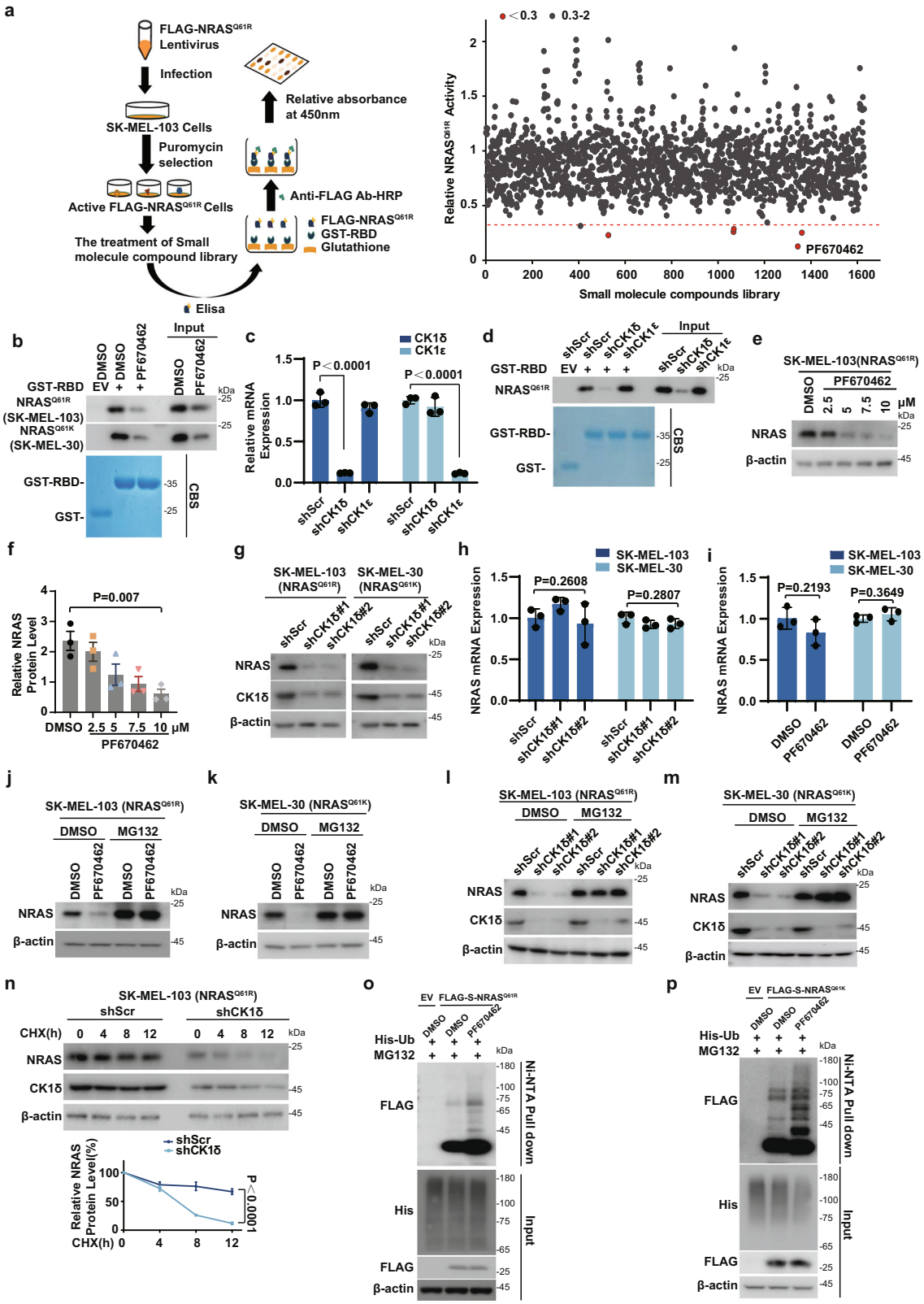

indicating that CK1δ could not act on NRAS Q61R directly and an unidentified factor might be critically involved. To identify the missing linker between CK1δ and NRAS Q61R, we performed tandem affinity purification and mass spectrometry analysis by utilizing SK-MEL-103 cells stably expressing FLAG-S-NRAS Q61R and identified the deubiquitinase USP46 as a potential interactor of NRAS Q61R (Fig. 3b). The endogenous interaction between USP46 and NRAS Q61R was validated in SK-MEL-103, SK-MEL-30 and SK-MEL-2 cells, respectively (Fig. 3c, d and Supplementary Fig. 3a). We also examined the interaction between purified USP46 and different NRAS mutants. As shown in Fig. 3e, purified GST-USP46 interacted with the NRAS Q61R and NRAS Q61K mutant more strongly than NRAS WT and Q61L. We also modeled the structure of ubiquitinated NRAS in complex with USP46 using protein-protein docking (Schrödinger, LLC, New York, NY, 2023) based on the

Fig. 1 | CK1δ positively regulates the activity of oncogenic NRAS mutants by affecting their protein stability. a Active NRAS chemiluminescence assay was performed to screen compounds mitigating the NRAS Q61R-Raf-RBD interaction. **b** The NRAS-Raf-RBD interaction in SK-MEL-103 (NRAS Q61R) and SK-MEL-30 (NRAS Q61K) cells pretreated with DMSO or PF670462 (10 μM) was examined by GST pull-down assay. Raf-RBD-bound NRAS (active NRAS fraction) and total NRAS in lysates were detected. **c** *CK1δ* and *CK1ε* mRNA levels in SK-MEL-103 cells expressing shScramble (shScr), shCK1δ or shCK1ε were determined by qRT-PCR. **d** The NRAS-Raf-RBD interaction in cells (**c**) was examined. **e**, **f** SK-MEL-103 cells were treated with DMSO or PF670462 for 24 h and western blotting was performed (**e**). NRAS protein level relative to β-actin was measured by Image J (**f**). **g** Cells expressing shScr or shCK1δ (#1 and #2) were generated and western blotting was performed. **h** *NRAS* mRNA levels in cells (**g**) were determined by qRT-PCR. **i** Cells were treated with DMSO or PF670462 (5 μM) for 24 h. *NRAS* mRNA level was determined by qRT-PCR. SK-MEL-103 (**j**) and SK-MEL-30 (**k**) cells were pretreated with DMSO or PF670462 (5 μM) for 24 h, then treated with DMSO or MG132 (10 μM) for 10 h. Western blotting was performed. SK-MEL-103 (**l**) and SK-MEL-30 (**m**) cells expressing shScr or shCK1δ were treated with DMSO or MG132 for 10 h and western blotting was performed. **n** Cycloheximide pulse-chase assay was performed in SK-MEL-103 cells expressing shScr or shCK1δ. NRAS protein levels relative to β-actin was measured by Image J. Cells were cotransfected with empty vector (EV), pIRES-NRAS Q61R (**o**), pIRES-NRAS Q61K (**p**) and other plasmids. Cells were pretreated with DMSO or PF670462 for 24 h and then treated with MG132 for 10 h. His-tagged ubiquitin was pulled-down by Ni-NTA beads and polyubiquitylated NRAS were examined. Immunoblots are representative of three independent experiments (**e**, **g**, **l**, **n**). Data were presented as mean ± SD of three independent experiments (**c**, **h**, **i**). Data were analyzed by two-sided Student's *t* test in (**i**, **n**), by two-sided one-way ANOVA in (**c**, **f**, **h**). Source data are provided as a Source Data file.

USP46-UB complex structure (PDB ID: 5CVM) and NRAS Q61K (PDB ID: 8VM2). The modeled structure revealed that K61 of NRAS is positioned near the groove formed by V91, V332, and E333 of USP46. The basic amino acids K61 and R61 could form a salt bridge with the acidic residue E333 of USP46, thereby enhancing the interaction between USP46 and NRAS Q61K/R mutants. Interestingly, a recent report has shown that NRAS Q61R and Q61K mutations exhibit a specific targetable pocket between Switch-II and α-helix 3, whereas the NRAS Q61L non-polar mutation category shows a different targetable pocket[23]. These findings suggest that different NRAS Q61 mutations can induce distinct local conformational changes and charge alterations, significantly affecting interactions with other proteins (Supplementary Fig. 3b). Additionally, purified GST-USP46 interacted with the NRAS Q61R mutant much more strongly than KRAS WT, HRAS WT and their mutants (Supplementary Fig. 3c, d). Similarly, the interaction of USP46 and NRAS Q61R is much stronger than NRAS WT pretreated with GDP or GTPγS (Fig. 3f). These results indicate that USP46 has a higher affinity with oncogenic NRAS mutants that could lock NRAS in an active state.

USP46 deubiquitinates and stabilizes oncogenic NRAS mutants

The direct interaction of USP46 and NRAS mutants prompt us to examine whether USP46 is essential to regulate the stability and oncogenic function of NRAS mutants. We found that the knockdown of USP46 in SK-MEL-103, SK-MEL-30 and SK-MEL-2 cells significantly decreased the protein level of NRAS mutants (Fig. 4a and Supplementary Fig. 4a). The depletion of USP46 did not affect *NRAS* mRNA level (Fig. 4b), while MG132 rescued the decreased protein level of NRAS mutants in USP46-depleted cells (Fig. 4c, d and Supplementary Fig. 4b). In line with these observations, NRAS mutant was less stable in cells depleting USP46 assessed by cycloheximide pulse-chase assay (Fig. 4e). And USP46 WT but not its catalytically inactive mutant C44S dramatically decreased the ubiquitination level of NRAS Q61R/K (Fig. 4f–h). In addition, a significant decrease of polyubiquitinated NRAS Q61R was observed when incubated with purified GST-USP46 WT rather than the C44S mutant in vitro (Fig. 4i). Conversely, the depletion of USP46 in SK-MEL-103 cells markedly increased the ubiquitination level of NRAS Q61R (Fig. 4j). We also examined the effect of USP46 on KRAS mutants and found that the depletion of USP46 hardly affected the protein level of KRAS mutants in KRAS-mutant NSCLC, pancreatic cancer, colorectal cancer cells (Supplementary Fig. 4c–e), which was consistent the inability of USP46 WT to affect the ubiquitination levels of KRAS and HRAS mutants (Supplementary Fig. 4f, g). Next, the effect of USP46 on NRAS WT were investigated. As shown in Supplementary Fig. 4h, i, the protein level of NRAS WT was not significantly affected by the depletion of USP46 in A375 and A2058, two melanoma cell lines harboring NRAS WT, since USP46 WT failed to affect the ubiquitination of NRAS WT. Intriguingly, the half-life of NRAS Q61R mutant was significantly longer than that of NRAS WT in SK-MEL-103 cells (Supplementary Fig. 4j). Together, these results indicate that USP46 specifically deubiquitinates and stabilizes NRAS Q61R/K mutants in melanoma but not NRAS WT, KRAS WT, HRAS WT and their mutants.

We next examined the specific ubiquitin linkage of NRAS mutants cleaved by USP46. As shown in Supplementary Fig. 5a, b, NRAS Q61R could be strongly ubiquitinated through both K48- and K63-specific polyubiquitin chains, while USP46 only catalyzed the cleavage of K48, but not K63-specific polyubiquitin chain. We next introduced point mutation into NRAS Q61R at several putative ubiquitination sites according to a previous report[24] and PhosphoSitePlug database. As shown in Supplementary Figs. 3b and 5c, d, the single mutant K135R or K147R could moderately decreased the ubiquitination of NRAS Q61R mutant, while the double mutant K135R/K147R largely abrogated the ubiquitination of NRAS Q61R and significantly increased its stability. We next generated several NRAS Q61R mutants containing one single intact lysine residue with the replacement of the other K to R. As shown in Fig. 4k, USP46 WT could dramatically decrease the ubiquitination level of K135 and K147 mutants. Lewis Cantley group previously reported that the monoubiquitination of K147 in KRAS WT in HEK293T cells could significantly affect GTP loading and its binding affinity to GST-RBD. In addition, the KRAS K147R and K147A mutations could enhance GTP loading, meanwhile the K147L mutant reduces the binding affinity to GST-RBD compared to the mono-ubiquitinated KRAS WT[25]. Thus, we investigate the potential effects of K147R and K147L mutations on NRAS mutant. As shown in Supplementary Fig. 5e, f, the K147R or K147L mutations could similarly decrease the ubiquitination of the NRAS Q61R mutant, and significantly increase its stability. These results suggest that USP46 stabilizes NRAS mutants by selectively deubiquitinating K48-specific polyubiquitin chain at K135 and K147.

USP46 promotes melanocyte malignant transformation and tumor progression through stabilizing NRAS mutants

We next investigate whether USP46 promotes tumorigenesis and progression of melanoma harboring NRAS Q61R/K mutants. As shown in Fig. 5a, the depletion of USP46 in genetically engineered human immortalized melanocytes (hTERT/CDK4^{R24C}/p53^{DD})[15] expressing NRAS Q61R significantly decreased the protein level of NRAS and suppressed the activation of downstream pathways assessed by p-AKT and p-ERK. Consistently, the depletion of USP46 substantially inhibited cell proliferation of NRAS Q61R-transformed melanocytes in vitro and in vivo (Fig. 5b–d), whereas the depletion of USP46 in cells expressing FLAG-NRAS Q61R-2KR did not exert these effects (Supplementary Fig. 6a–d). These results indicate the pivotal role of USP46 in oncogenic NRAS-driven melanomagenesis. As shown in Supplementary Fig. 6e, the depletion of USP46 in genetically engineered human immortalized melanocytes (hTERT/CDK4^{R24C}/p53^{DD}) expressing NRAS Q61R induced a significant reduction of cell proliferation as assessed by Ki67 staining, and a significant increase of apoptotic cell death as assessed by cleaved caspase-3 staining. In addition, the reconstitution of USP46 WT rather

https://doi.org/10.1038/s41467-024-54140-1

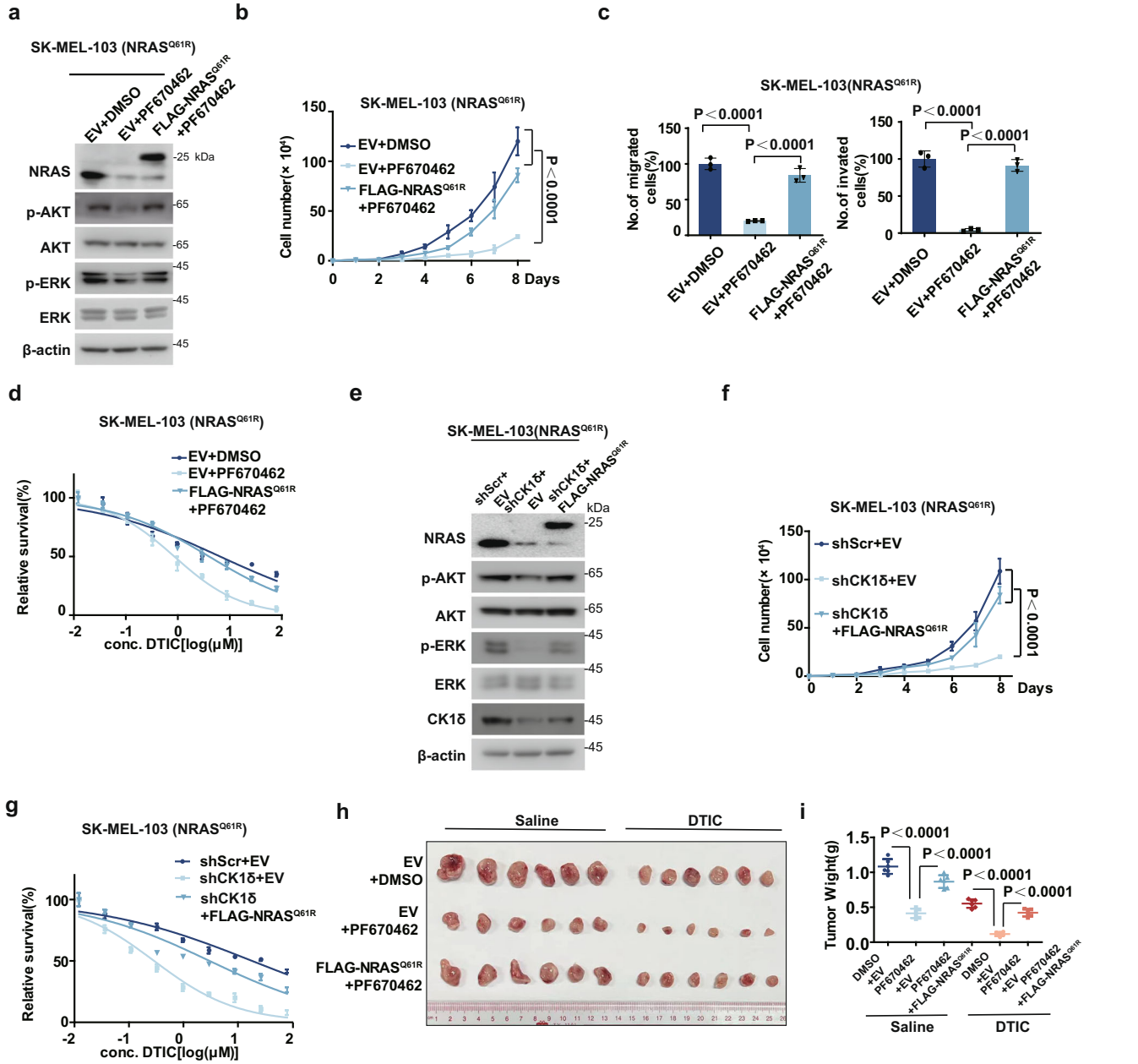

Fig. 2 | CK1δ promotes tumor progression through stabilizing NRAS mutants. **a** SK-MEL-103 cells were transfected with empty vector or FLAG-NRAS Q61R and treated with DMSO or PF670462 (5 μM) for 24 h. Western blotting was performed with indicated antibodies. **b** Cell proliferation assay was performed from cells in (**a**). **c** The migration and invasion abilities of cells as in (**a**) were measured by Transwell migration and invasion assays. **d** Cells as in (**a**) were treated with DMSO or indicated concentrations of dacarbazine (DTIC) and cell survival was determined. **e** SK-MEL-103 cells stably expressing shScramble (shScr) or shCK1δ were transfected with empty vector or indicated plasmids. Western blotting was performed with indicated antibodies. **f** Cell proliferation of cells in (**e**) was examined. **g** Cells as in (**e**) were treated with indicated concentrations of DTIC and cell survival was determined. The results represent mean ± s.d. from three independent experiments. **h**, **i** Cells as in (**a**) were subcutaneously implanted into nude mice (5–6 weeks, $n = 6$). When tumors reached around 150–200 mm^3 in size, mice were treated with saline, PF670462 (4 mg/kg), dacarbazine (8 mg/kg) or PF670462 plus dacarbazine. Tumors were collected (**h**) and weights were measured (**i**). The results represent the mean ± s.d. of data from six mice. Data were presented as mean ± SD of three independent experiments (**b**–**d**, **f**, **g**). Data were analyzed by two-sided one-way ANOVA in (**b**, **c**, **f**, **i**). Source data are provided as a Source Data file.

than the inactive C44S mutant in endogenous USP46-deficient melanocytes dramatically restored p-AKT and p-ERK, the colony formation capacity, as well as the tumor-forming ability of NRAS Q61R transformed melanocytes in vitro and in vivo (Fig. 5e–h). As shown in Supplementary Fig. 6f, the reconstitution of USP46 WT but not the inactive C44S mutant could rescue the alterations of Ki67 and cleaved caspase-3 expression caused by the depletion of USP46. Furthermore, the depletion of USP46 in SK-MEL-103, SK-MEL-30 and SK-MEL-2 cells significantly suppressed levels of p-AKT and p-ERK, cellular proliferation, migration and invasion abilities along with increased cellular sensitivity to DTIC, whereas the reconstitution of NRAS Q61R/K, NRAS Q61R-K135R + K147R or NRAS Q61R-K135R + K147L in USP46-deficient cells markedly rescue such effects (Fig. 5i–l and Supplementary Figs. 6g–j and 7a–f). In the line with these results in vitro, similar results were observed in xenograft animal experiments (Fig. 5m, n and Supplementary Fig. 7g, h). We also found that the depletion of USP46 in SK-MEL-103 cells dramatically reduced Ki67 expression along with upregulated cleaved caspase-3 staining in tumors from

https://doi.org/10.1038/s41467-024-54140-1

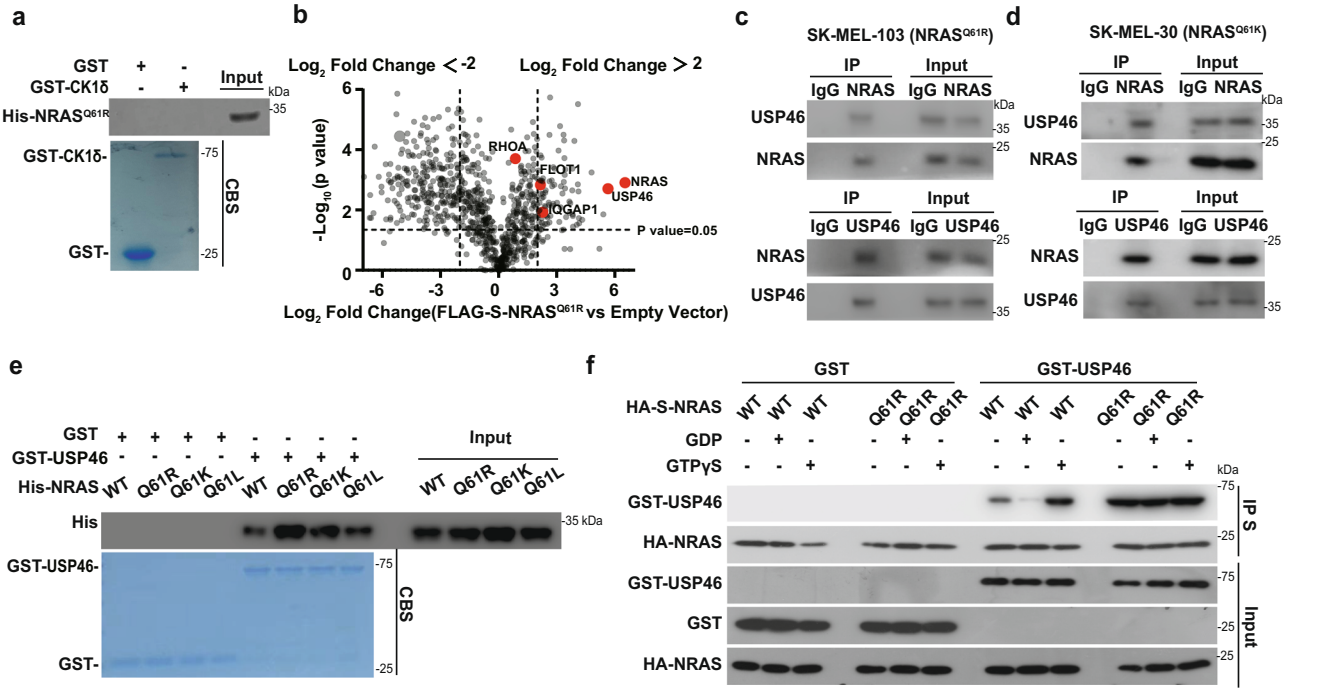

Fig. 3 | USP46 binds oncogenic NRAS mutants. a Purified recombinant His-NRAS Q61R were incubated with GST or GST-CK1δ and the direct interaction between CK1δ and NRAS Q61R was examined. CBS Coomassie blue staining. **b** Volcano plots of NRAS Q61R-associated proteins identified by mass spectrometric analysis. SK-MEL-103 cells stably expressing FLAG-S-NRAS Q61R or Empty Vector were generated and treated with MG132 (10 μM) for 10 h. NRAS Q61R or Empty Vector immunoprecipitates were subjected to mass spectrometric analysis ($n = 3$). Cell lysates of SK-MEL-103 (**c**) and SK-MEL-30 (**d**) were subjected to immunoprecipitation with IgG, anti-NRAS or anti-USP46 antibodies, respectively. Western blotting was performed with indicated antibodies. **e** Purified recombinant GST, GST-USP46 and His-NRAS WT, His-NRAS Q61R, His-NRAS Q61K and His-NRAS Q61L were incubated in vitro as indicated. The interaction between USP46 and NRAS was examined. CBS Coomassie blue staining. **f** Cells were transfected with pLV5-NRAS WT or NRAS Q61R (containing HA and S tag). NRAS was pull-downed by S-protein agarose, preloaded with DMSO, 1 mM GDP or GTPγS and incubated with purified GST or GST-USP46. Western blotting was performed with indicated antibodies. Source data are provided as a Source Data file.

mice treated with saline or DTIC, although the phenotypical alterations were much more obvious in DTIC-treated group. Moreover, the reconstitution of NRAS Q61R significantly rescued such effects caused by the depletion of USP46 (Supplementary Fig. 7i). In addition, effects of NRAS Q61R or the ubiquitination-deficient NRAS mutant (NRAS Q61R-2KR) on USP46-depleted melanoma cells were examined. Compared to control cells (shScramble), the depletion of USP46 in SK-MEL-103 cells expressing FLAG-NRAS Q61R markedly decreased the protein level of the NRAS mutant, inhibited the activation of downstream pathways assessed by p-AKT and p-ERK, reduced cell proliferation, and increased cellular sensitivity to DTIC. However, the depletion of USP46 did not exert such effects in SK-MEL-103 cells expressing FLAG-NRAS Q61R-2KR (Supplementary Fig. 8a–c). Conversely, the overexpression of USP46 WT rather than USP46 C44S in SK-MEL-103 cells and SK-MEL-30 cells markedly increased the protein level of NRAS mutant and NRAS mutant-dependent malignant phenotypes (Supplementary Fig. 8d–f). These results reveal the tumor-promoting activity of USP46 in melanoma is mainly through deubiquitinating and stabilizing NRAS Q61R/K mutants.

CK1δ binds and phosphorylates USP46 at Thr209, Ser351 and Ser354

Since both CK1δ and USP46 stabilize NRAS mutants by inhibiting its ubiquitination and subsequent degradation, it is tempting to speculate that USP46 might be the potential linker between CK1δ and NRAS mutants. Interestingly, we also identified CK1δ as a major USP46-associated protein by tandem affinity purification and mass spectrometry analysis using SK-MEL-103 cells stably expressing FLAG-USP46 (Fig. 6a). The endogenous USP46-CK1δ interaction were validated in SK-MEL-103 and SK-MEL-30 cells, respectively (Fig. 6b and Supplementary Fig. 9a). In addition, purified GST-CK1δ protein could pull-down His-USP46 in a cell-free system, indicating the direct interaction between CK1δ and USP46 (Fig. 6c). We next investigated whether CK1δ could phosphorylate USP46. CK1δ-mediated phosphorylation of USP46 in the in vitro kinase assay was detected by using phospho-tag gel, which was significantly mitigated by the treatment of PF670462 (Fig. 6d). To identify potential phosphorylation sites of USP46 by CK1δ, we analyzed the amino acid sequence of USP46 and found that Thr209, Ser351 and Ser354 match with CK1 consensus phosphorylation motif[26] and are highly conserved among multiple species (Supplementary Fig. 9b). The single mutation of USP46 T209A, S351A or S354A only mildly decreased the phosphorylation of USP46, while the 3A mutant (T209A/S351A/S354A) almost completely abolished it assessed by phospho-tag gel (Fig. 6e). Furthermore, the in vitro kinase assay was performed by using anti-p-Ser and anti-p-Thr antibodies to examine the phosphorylation of USP46 isolated from SK-MEL-103 cells stably expressing pLVX3-GST-USP46 WT and the 3A mutant. As shown in Supplementary Fig. 9c, CK1δ significantly increased the phosphorylation of USP46 WT assessed by anti-p-Ser and anti-p-Thr antibodies, whereas the 3A mutant could largely decrease such phosphorylation events. This result suggests that CK1δ could regulate the phosphorylation of USP46 at Thr209, Ser351 and Ser354 residues, which all contain the S/T-X-X-S/T motif. Intriguingly, some basal phosphorylation of isolated USP46 from SK-MEL-103 cells was noticed even in the absence of CK1δ, indicating that other protein kinases might also contribute to the phosphorylation of USP46. Considering that CLK1, Creatine Kinase B (CKB), Aurora kinase B (AURKB), PKN2 and several other serine/threonine protein kinases were identified as potential interactors of USP46 in our mass spectrometry analysis of FLAG-S-tagged USP46 (Fig. 6a), making it possible that certain

https://doi.org/10.1038/s41467-024-54140-1

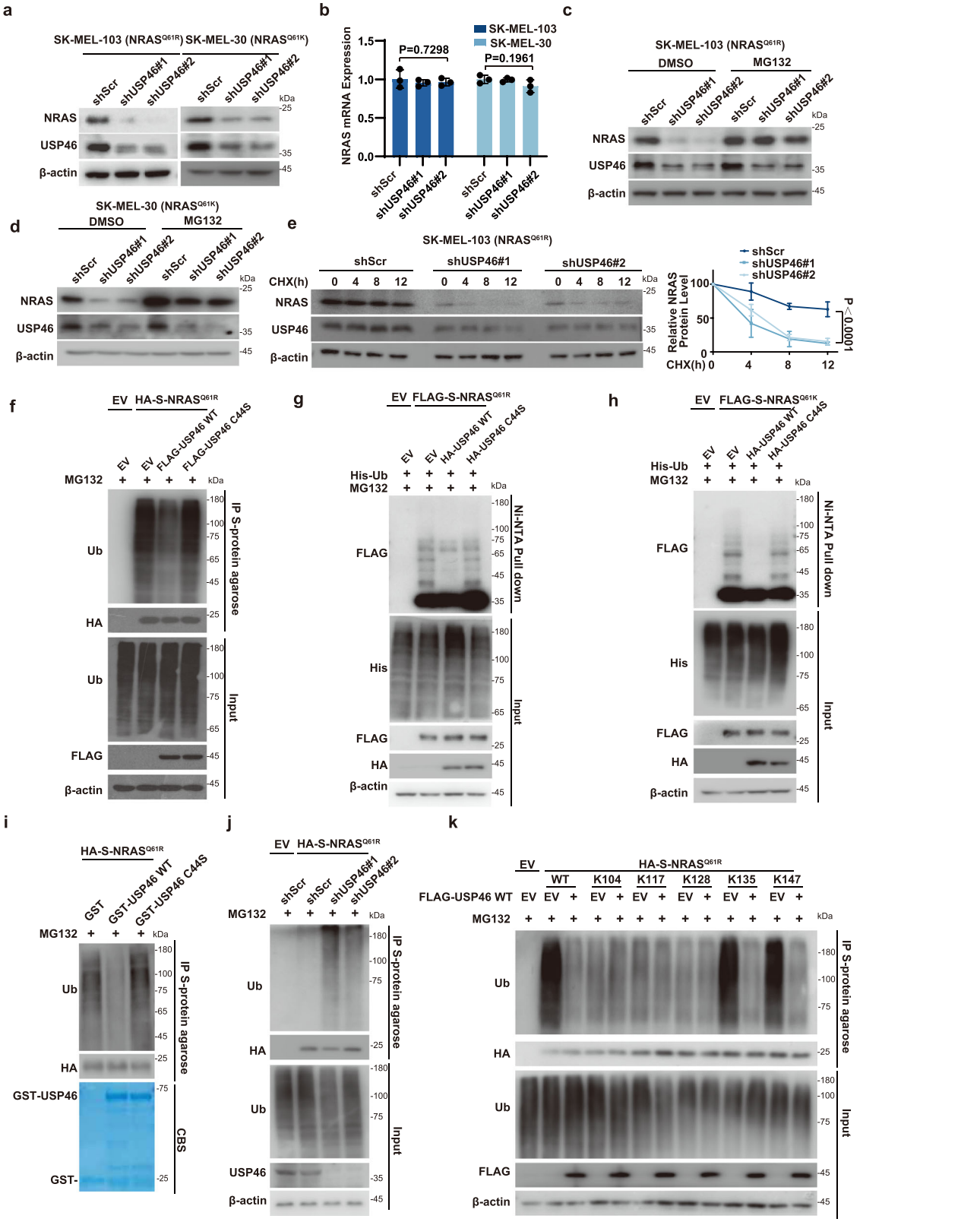

USP46-associated kinases might mediate potential priming phosphorylation in these consensus sequences of USP46.

We next investigated whether CK1δ-mediated phosphorylation affect the enzymatic activity USP46 toward NRAS mutants. Compared to USP46 WT, the reconstitution of single mutant of USP46 T209A, S351A or S354A could partially rescue the reduced protein level of NRAS Q61R induced by endogenous USP46-deficiency, while the 3 A mutant failed to do so (Fig. 6f). In addition, the ability of the single mutant to cleave the ubiquitination of NRAS Q61R is moderately weaker than USP46 WT, while the 3 A mutant largely impaired the ability to deubiquitinate NRAS Q61R efficiently (Fig. 6g). These results suggest that CK1δ directly phosphorylates USP46 and activates its deubiquitinase activity toward NRAS Q61R.

Fig. 4 | USP46 deubiquitinates and stabilizes NRAS activation mutants. a USP46 and NRAS protein levels in SK-MEL-103 and SK-MEL-30 cells expressing shScramble (shScr) or shUSP46 (#1 and #2) were measured by western blotting. **b** *NRAS* mRNA levels in cells (**a**) was determined by qRT-PCR. SK-MEL-103 (**c**) and SK-MEL-30 (**d**) cells expressing shScramble (shScr) or shUSP46 were treated with DMSO or MG132 (10 μM) for 10 h and western blotting was performed. **e** Cycloheximide pulse-chase assay was performed in cells (**a**); NRAS protein levels relative to β-actin was measured by Image J. **f** SK-MEL-103 cells were cotransfected with empty vector (EV), pLV5-NRAS Q61R (containing HA and S tag), FLAG-USP46 WT or FLAG-USP46 C44S mutant, then treated with MG132 for 10 h. NRAS Q61R was pull-downed by S-protein agaroses and polyubiquitylated NRAS Q61R was detected. SK-MEL-103 and SK-MEL-30 cells were cotransfected with empty vector, pIRES-NRAS Q61R (**g**), pIRES-NRAS Q61K (**h**) (containing FLAG and S tag) and other indicated plasmids. His-tagged ubiquitin was pulled-down by Ni-NTA beads and polyubiquitylated NRAS Q61R/K protein was examined. **i** SK-MEL-103 cells were transfected with empty vector or pLV5-NRAS Q61R (containing HA and S tag) and treated with MG132 (10 μM) for 10 h. NRAS Q61R was pull-downed by S-protein agaroses and incubated with purified GST, GST-USP46 WT or GST-USP46 C44S at 4 °C for 24 h. Polyubiquitylated NRAS Q61R was examined. **j** SK-MEL-103 cells expressing shScramble (shScr) or shUSP46 were transfected with empty vector or indicated plasmids followed by MG132 treatment for 10 h. NRAS Q61R was pull-downed by S-protein agarose and polyubiquitylated NRAS Q61R was examined. **k** Cells expressing empty vector, pLV5-NRAS Q61R, K104, K117, K128, K135 or K147 mutants (containing HA and S tag) were transfected with empty vector or FLAG-USP46 and treated with MG132 (10 μM) for 10 h. NRAS Q61R was pull-downed by S-protein agarose and polyubiquitylated NRAS Q61R was examined. Immunoblots are representative of three independent experiments (**a**, **e**). Data were presented as mean ± SD of three independent experiments (**b**). Data were analyzed by two-sided one-way ANOVA in (**b**, **e**). Source data are provided as a Source Data file.

CK1δ-mediated phosphorylation of USP46 regulates tumor progression of oncogenic NRAS-driven melanoma

We further tested whether USP46 is the missing link between CK1δ and NRAS mutants. As shown in Fig. 7a, b, the depletion or inhibition of CK1δ by PF670462 could not further decrease the protein level of NRAS mutant in USP46-deficent cells. In addition, the overexpression of USP46 WT in SK-MEL-103 and SK-MEL-30 cells significantly increased the protein level of NRAS mutants, which could be largely mitigated by the treatment of PF670462 (Fig. 7c and Supplementary Fig. 10a). To rule out the non-specific effect of PF670462, two different CK1δ inhibitors D4476 and Casein kinase 1δ-IN-8 were used to treat SK-MEL-103 and SK-MEL-30 cells. As shown in Supplementary Fig. 10b–e, the overexpression of USP46 WT in SK-MEL-103 and SK-MEL-30 cells increased the protein level of NRAS mutants, which could be largely mitigated by the treatment of D4476 or Casein kinase 1δ-IN-8. And the treatment of D4476 and Casein kinase 1δ-IN-8 did not affect the levels of p-p38 and p-EGFR in SK-MEL-103 and SK-MEL-30 cells. Consistently, the overexpression of USP46 WT dramatically decreased the ubiquitination level of NRAS Q61R, which was markedly abrogated by the depletion or inhibition of CK1δ by PF670462 or Casein kinase 1δ-IN-8 rather than β-catenin inhibitor MSAB (Fig. 7d, e and Supplementary Fig. 10f).

Next, we examined the effect of CK1δ-mediated phosphorylation of USP46 on the ubiquitination of NRAS mutants. As shown in Fig. 7f, g, the overexpression of USP46 WT could dramatically decrease the ubiquitination level of NRAS mutants, whereas the 3 A mutant failed to do so. In addition, the reduced protein level of NRAS Q61R in USP46-deficient SK-MEL-103 cells could be largely rescued by the reconstitution of USP46 WT, but not the 3 A mutant (Fig. 7h). Moreover, the reconstitution of USP46 WT in endogenous USP46-deficient SK-MEL-103 cells dramatically increased the half-life of NRAS mutant compared to the 3 A mutant (Fig. 7i). These results indicate that CK1δ stabilizes NRAS mutant in melanoma in a USP46-dependent manner.

We next investigated the function of CK1δ-mediated phosphorylation of USP46 on oncogenic NRAS-dependent malignant processes. As shown in Fig. 7j and Supplementary Fig. 10g, the overexpression of USP46 WT, but not the 3 A mutant in SK-MEL-103, SK-MEL-30 and SK-MEL-2 cells significantly increased the protein level of NRAS mutants and levels of p-AKT and p-ERK. And the reconstitution of USP46 WT but not the 3 A mutant in endogenous USP46-deficient SK-MEL-103 cells and SK-MEL-2 cells significantly increased the proliferation, migration and invasion abilities along with decreased cellular sensitivity to DTIC in vitro and in vivo (Fig. 7k–o and Supplementary Fig. 10h, i). Moreover, the suppressive effects of targeting CK1δ by PF670462 were observed in cells reconstituted with USP46 WT, but not the 3 A mutant. These results indicate that CK1δ-mediated phosphorylation of USP46 is pivotal to stabilize NRAS mutant and promote oncogenic NRAS-dependent tumor progression.

The expression of NRAS Q61R/K positively correlates with USP46 and CK1δ in melanoma

We further examine the clinical relevance of this axis by analyzing protein expression of CK1δ, USP46 and NRAS in melanoma samples harboring NRAS Q61R/K by immunohistochemistry. As shown in Fig. 8a, b, the levels of CK1δ and USP46 were positively correlated with the expression level of NRAS mutant in melanoma harboring with NRAS Q61R (19 cases) and NRAS Q61K (16 cases). Overall, our study demonstrates that the CK1δ-USP46 axis functions as an important regulatory mechanism to control the stabilization of NRAS Q61R/K mutants and provides an appealing therapeutic strategy in oncogenic NRAS-driven melanoma (Fig. 8c).

Discussion

Compared to non-NRAS mutated melanoma, oncogenic NRAS-driven melanomas are more aggressive with higher metastasis rates, poorer outcomes and lower median survival[27]. The management of melanomas harboring NRAS mutations remains challenging. While immunotherapy has offered significant advancements for various subtypes of melanoma[28], it is limited by the outcome variability between patients and side effects. There remains a critical unmet need for innovative treatments for NRAS-mutant melanoma, particularly for metastatic cases. Currently, a variety of treatment approaches has been explored in the preclinical and clinical trials, primarily focusing on inhibiting the MAPK signaling pathway[29], either alone or in combination with interventions targeting downstream signaling pathways of NRAS, such as CDK4/6, FAK, and autophagy pathways[30–33]. However, the efficacy of these approaches has been limited by diverse resistance mechanisms. These include the reactivation of MAPK signaling and activation of multiple pro-survival pathways such as mTOR1/2 signaling mTOR-S6 signaling, Rho/MRTF pathway, MITF pathway, the enhanced activity of Bcl-2, and the activation of metabolic enzyme PHGDH[34–37]. In this study, we reveal several unexpected findings with important clinical implications for the treatment of NRAS mutant melanoma. First, we identify the CK1δ-USP46 axis as an uncharacterized upstream regulator of NRAS Q61R/K mutants. Mechanistically, CK1δ-mediated phosphorylation of USP46 is a critical post-translational mechanism that controls stability and oncogenic function of these NRAS mutants. We provide preclinical evidence demonstrating that targeting CK1δ and USP46 is an effective approach to suppress tumor progression of melanoma carrying NRAS Q61R/K mutants (Fig. 8c).

Considering the challenge in developing inhibitors directly targeting NRAS, developing alternative therapeutic strategies such as controlling stability of oncogenic NRAS mutants would benefit the clinical outcome of NRAS-mutant melanoma. Emerging evidence suggests that ubiquitination and subsequent degradation play important roles in regulating RAS stability and activity. HRAS can be ubiquitinated and degraded by the E3 ligase β-TrCP, and aberrant

https://doi.org/10.1038/s41467-024-54140-1

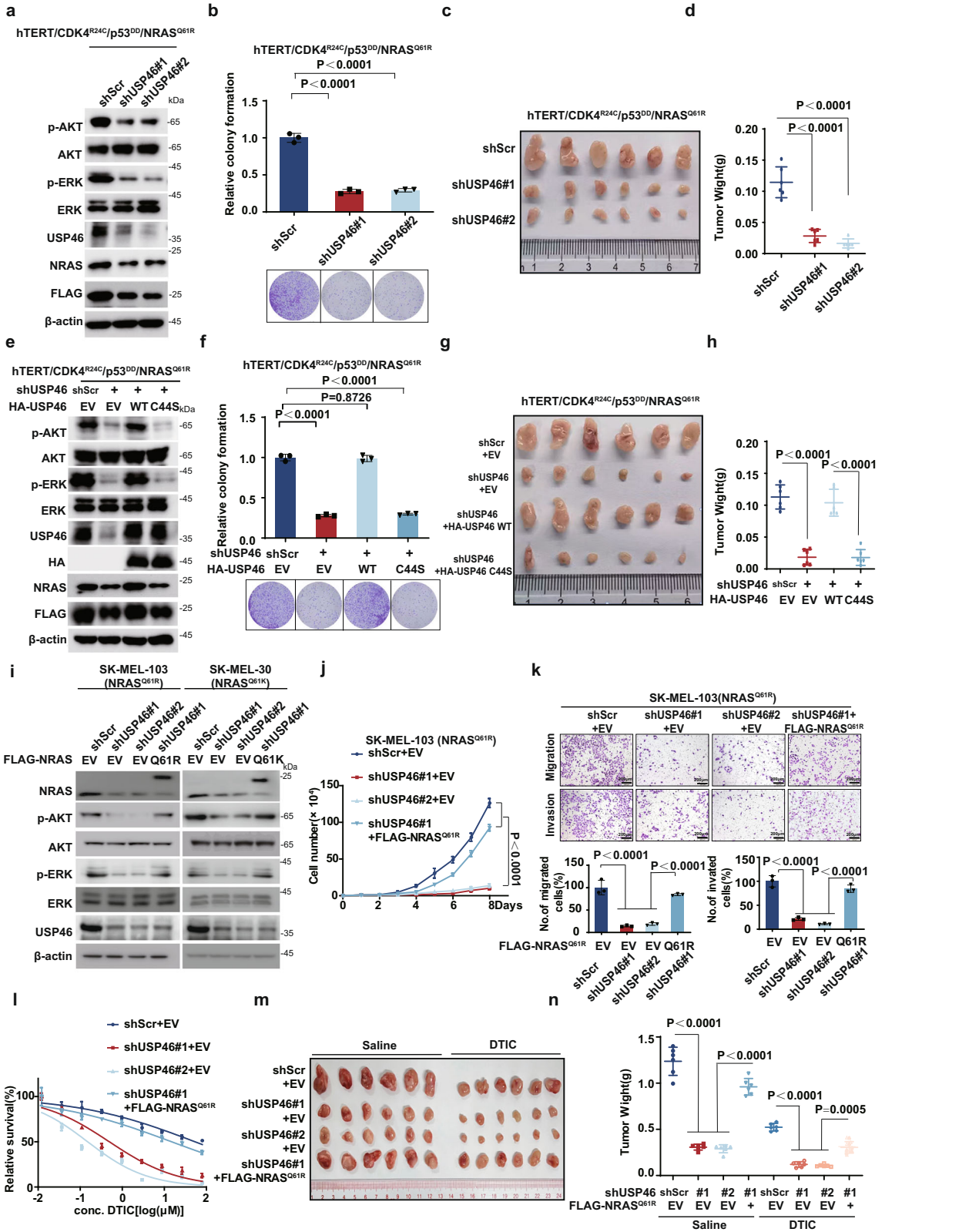

activation of Wnt/β-catenin signaling promotes intestinal tumorigenesis by stabilizing HRAS[38]. OTUB1 triggers the activation of MAPK pathway by inhibiting RAS ubiquitination, which in turn promotes the development of lung cancer[39]. In our study, we screened the protein kinase CK1δ as a critical regulator that stabilizes oncogenic NRAS mutant through an active NRAS chemiluminescence assay. Although CK1δ is implicated in neurodegenerative diseases and certain cancers[12,40,41], its role in melanoma remains poorly understood. Analysis of datasets from tumor cell lines and tumor tissues revealed elevated expression of CK1δ in many cancer types, including melanoma, indicating the potential involvement of CK1δ in melanoma[42]. However, Sinnberg et al. reported that CK1δ is not substantially involved in melanoma progression since the depletion of CK1δ by one siRNA does not significantly affect the growth and survival of metastatic

https://doi.org/10.1038/s41467-024-54140-1

Fig. 5 | USP46 promotes melanocyte malignant transformation and tumor progression through stabilizing NRAS mutants. a hTERT/CDK4^{R24C}/p53^{DD} human melanocytes expressing FLAG-NRAS Q61R were infected with lentivirus encoding shScramble (shScr) or shUSP46 (#1 and #2) and indicated proteins were examined by western blotting. **b** The colony formation ability of hTERT/CDK4^{R24C}/p53^{DD} melanocytes as in (**a**) was measured. **c**, **d** Cells as in (**a**) were subcutaneously implanted into nude mice (5–6 weeks, $n = 6$). Tumors were collected (**c**) and tumor weights were analyzed (**d**). **e** Cells as in (**a**) were transfected with empty vector (pLV5), USP46 WT or C44S mutant and western blotting was performed with indicated antibodies. **f** The colony formation assay of melanocytes as in (**e**) was performed. **g**, **h** Cells as in (**e**) were subcutaneously implanted into nude mice (5–6 weeks, $n = 6$). Tumors were collected (**g**) and weights were measured (**h**). **i** SK-MEL-103 cells stably expressing shScramble (shScr) or shUSP46 (#1 and #2) were transfected with empty vector (pLV3) or FLAG-NRAS Q61R and western blotting was performed with indicated antibodies. **j** Cell proliferation of SK-MEL-103 cells in (**i**) was examined. **k** The migration and invasion abilities of SK-MEL-103 as in (**i**) were measured by Transwell migration and invasion assays and results were quantified in low panel. **l** SK-MEL-103 cells as in (**i**) were treated with indicated concentrations of dacarbazine (DTIC) and cell survival was determined. **m**, **n** SK-MEL-103 cells as in (**i**) were subcutaneously implanted into nude mice (5–6 weeks, $n = 6$). When tumors reached around 150–200 mm^3 in size, mice were treated with saline or DTIC (8 mg/kg). Tumors were collected (**m**) and weights were measured (**n**). The results represent the mean ± s.d. of data from six mice. Data were presented as mean ± SD of three independent experiments (**b**, **f**, **j**–**l**). Data were analyzed by two-sided one-way ANOVA in (**b**, **d**, **f**, **h**, **j**, **k**, **n**). Source data are provided as a Source Data file.

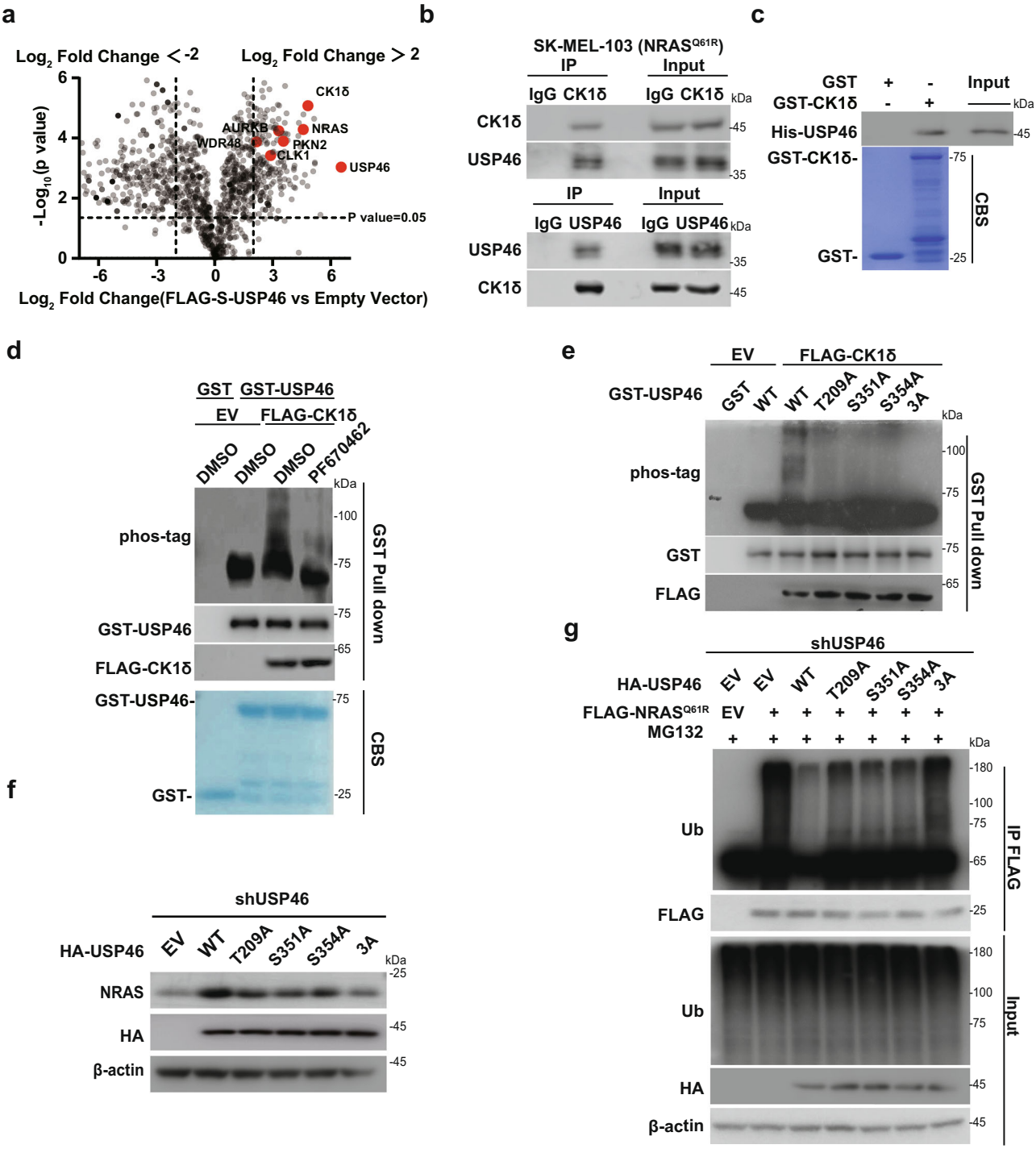

Fig. 6 | CK1δ binds and phosphorylates USP46 at Thr209, Ser351 and Ser354. **a** Volcano plots of USP46 associated proteins identified by mass spectrometric analysis. SK-MEL-103 cells stably expressing FLAG-S-USP46 or Empty Vector were generated and treated with MG132 (10 μM) for 10 h. USP46 or Empty Vector immunoprecipitate complexes were subjected to mass spectrometric analysis ($n = 3$). **b** SK-MEL-103 cell lysates were subjected to immunoprecipitation with IgG, anti-CK1δ or anti-USP46 antibodies. The immunoprecipitates were blotted with indicated antibodies. **c** Purified recombinant GST, GST-CK1δ and His-USP46 were incubated in vitro as indicated. The interaction between CK1δ and USP46 was examined. CBS, Coomassie blue staining. **d** SK-MEL-103 cells stably expressing empty vector or FLAG-CK1δ were generated. FLAG-CK1δ was immunoprecipitated with anti-FLAG affinity gel and incubated with GST or GST-USP46 protein purified from SK-MEL-103 cells stably expressing empty vector (pLVX3-GST) or pLVX3-GST-USP46 WT in an in vitro kinase buffer with the presence of DMSO or CK1δ inhibitor PF670462 (5 μM). The phosphorylation of USP46 was examined by western blotting using Phos-tag containing gel. **e** CK1δ phosphorylates USP46 at Thr209, Ser351 and Ser354. Cell lysates of SK-MEL-103 cells stably expressing FLAG-CK1δ were immunoprecipitated with anti-FLAG affinity gel and incubated with GST, GST-USP46 WT, the single mutants or the 3A mutants purified from SK-MEL-103 cells stably expressing empty vector (pLVX3-GST), pLVX3-GST-USP46 WT or indicated mutants in an in vitro kinase buffer. The phosphorylation of USP46 was assessed by western blotting using Phos-tag containing gel. **f** SK-MEL-103 cells stably expressing shUSP46 were transfected with empty vector (pLV5), USP46 WT or the phosphorylation defective mutant 1A and 3A and western blotting was performed with indicated antibodies. **g** Endogenous USP46-deficient SK-MEL-103 cells were transfected with empty vector (pLV5), HA-USP46, the single mutants, the 3A mutants or indicated plasmids and then treated with MG132 (10 μM) for 10 h. FLAG-NRAS Q61R was immunoprecipitated with anti-FLAG affinity gel and the ubiquitination of FLAG-NRAS Q61R were measured by western blotting. Source data are provided as a Source Data file.

melanoma cells in vitro[18]. Melanoma cells with BRAF mutations and NRAS WT as well as Scbl2 cell line carrying NRAS mutant were mainly used in Sinnberg et al.'s study. However, NRAS mutation in the Scbl2 cell line was the substitution of Leu (L) by a Gln (Q) acid at position 61 (Q61L) but not Q61K according to the information provided by the Cellosaurus. In our study, the interaction of USP46 with NRAS WT and Q61L mutant is weaker than NRAS Q61R or Q61K (Fig. 3e), which might be due to the conformation difference and charge alterations between the positively charged mutations (Q61R and Q61K) and non-polar mutation (Q61L). In addition, the effect of CK1δ inhibition on the ubiquitination of NRAS Q61R and Q61K mutants was more significant than on NRAS Q61L mutant (Fig. 1o, p and Supplementary Fig. 1n–r). These results might explain the insignificant effect of CK1δ depletion or inhibition by PF670462 on the growth of Sbcl2 cells. In contrast to their findings in melanoma cells with BRAF mutations and NRAS WT as well as Scbl2 cell line carrying NRAS Q61L, our study reveals the tumor promoting activity of CK1δ in NRAS Q61R/K mutant driven melanoma based on the following evidence. First, the selective CK1δ/ε inhibitor PF670462 potently inhibits the active fraction of NRAS Q61R/K mutants (Fig. 1a, b). Second, CK1δ but not CK1ε is pivotal for the inhibitory effect of PF670462 on these NRAS mutants (Fig. 1c–g and Supplementary Fig. 1f, g). Third, the genetic ablation or pharmacological inhibition of CK1δ causes the degradation of NRAS Q61R/K by affecting their ubiquitination level (Fig. 1e–p and Supplementary Fig. 1n–q). Importantly, targeting CK1δ could significantly suppresses the activity of NRAS mutants and their mediated malignant phenotypes in vitro and in vivo (Fig. 2 and Supplementary Fig. 2a–d).

Intriguingly, the ability of CK1δ to stabilize NRAS mutants in melanoma is not through direct phosphorylation of NRAS, as no direct interaction between purified GST-CK1δ and His-NRAS Q61R was observed (Fig. 3a). Instead, the deubiquitinase USP46 functions as the linker between CK1δ and NRAS mutants based on following evidence. First, USP46 directly binds, deubiquitinates and stabilizes NRAS mutants in an enzymatic activity-dependent manner, thereby promoting melanomagenesis and tumor progression of melanoma harboring NRAS Q61R/K mutants (Figs. 3–5 and Supplementary Figs. 3–8). It is also noteworthy that we cannot rule out the possibility of additional mechanisms engaged in USP46-regulated tumor progression of oncogenic NRAS-driven melanoma since the ectopic expression of NRAS mutants could not completely rescue phenotypic changes caused by the depletion of USP46 (Fig. 5 and Supplementary Figs. 6–8). Second, CK1δ binds and regulates the phosphorylation of USP46 (Fig. 6 and Supplementary Fig. 9). Interestingly, we did notice some basal phosphorylation of isolated USP46 from SK-MEL-103 cells even in the absence of CK1δ (Supplementary Fig. 9c), indicating that other protein kinases might also contribute to the phosphorylation of USP46. In our mass spectrometry analysis of FLAG-S-tagged USP46, CLK1, Aurora kinase B (AURKB), PKN2, and several other serine/threonine protein kinases were identified as potential interactors of USP46 (Fig. 6a). As the phosphorylation of USP46 is poorly studied, the protein kinases other than CK1δ responsible for the basic phosphorylation of USP46 need further investigation in the future. Third, CK1δ-mediated phosphorylation is pivotal for the deubiquitinase activity of USP46 towards NRAS mutants and its dependent malignant phenotypes (Fig. 7d–g). The inhibition of such phosphorylation events by pharmacologically targeting CK1δ or the reconstitution of the phosphorylation-defective mutant USP46 3 A fails to promote the malignant features mentioned above (Fig. 7j–o and Supplementary Fig. 10g–i). Importantly, our histological analyses show that the expressions of CK1δ and USP46 are positively correlated with the expression of NRAS mutants in 35 cases of human melanoma specimens harboring NRAS Q61R/K. Further preclinical studies including PDX models and clinical studies are needed to explore the therapeutic benefits of targeting the CK1δ-USP46 axis in oncogenic NRAS mutant-driven melanoma.

Collectively, our findings reveal the potential therapeutic benefit of CK1δ inhibitors in suppressing melanoma with NRAS Q61R/K mutants. However, several critical considerations must be considered to understand its potential limitations and challenges. PF670462 is known to target both CK1δ and CK1ε isoforms, which share a significant degree of homology and are involved in the phosphorylation of a variety of proteins, including PER (impacting circadian rhythm)[43], DVL (Wnt signaling pathway)[40], as well as AMPA receptor (neuronal functions)[44]. Consequently, the use of PF670462 may lead to considerable effects beyond the intended therapeutic targets, potentially disrupting circadian rhythms, Wnt signaling, and neuronal processes. Moreover, the off-target inhibition of PF670462, including its action on PKAα, p38, MAP4K4, LCK, and EGFR[45], introduces additional complexity to its specificity and toxicity profile, highlighting the critical need for the development of more selective CK1δ inhibitors to minimize unintended effects.

The next question is how CK1δ is deregulated in NRAS-mutant melanoma. The transcription of CK1δ has been reported to be upregulated in some tumor types including breast cancer[12] and hepatocellular carcinoma[46], which significantly associate with poor clinical outcomes. However, the regulation of CK1δ in melanoma remains elusive. Stress conditions such as γ-irradiation and DNA-damaging agents have been reported to increase CK1δ transcription in a p53-dependent manner[10,47]. Unlike many solid tumors harboring p53 mutations, most melanomas retain wild-type p53 protein, which promotes migration-related cytokine expression and initiates a slow-cycling state, thereby driving therapy resistance in melanoma[48,49]. In addition, CK1δ can be phosphorylated by several kinase including PKCα and Chk1, which negatively regulate the activity of CK1δ in vitro[50–52]. Further efforts are warranted to investigate regulatory mechanisms of CK1δ aberrations and validate the effects of targeting CK1δ with more isoform-specific inhibitors on NRAS-mutant melanoma and other cancers such as acute myeloid leukemia, which harbors NRAS mutants at a relatively high frequency[53,54].

https://doi.org/10.1038/s41467-024-54140-1

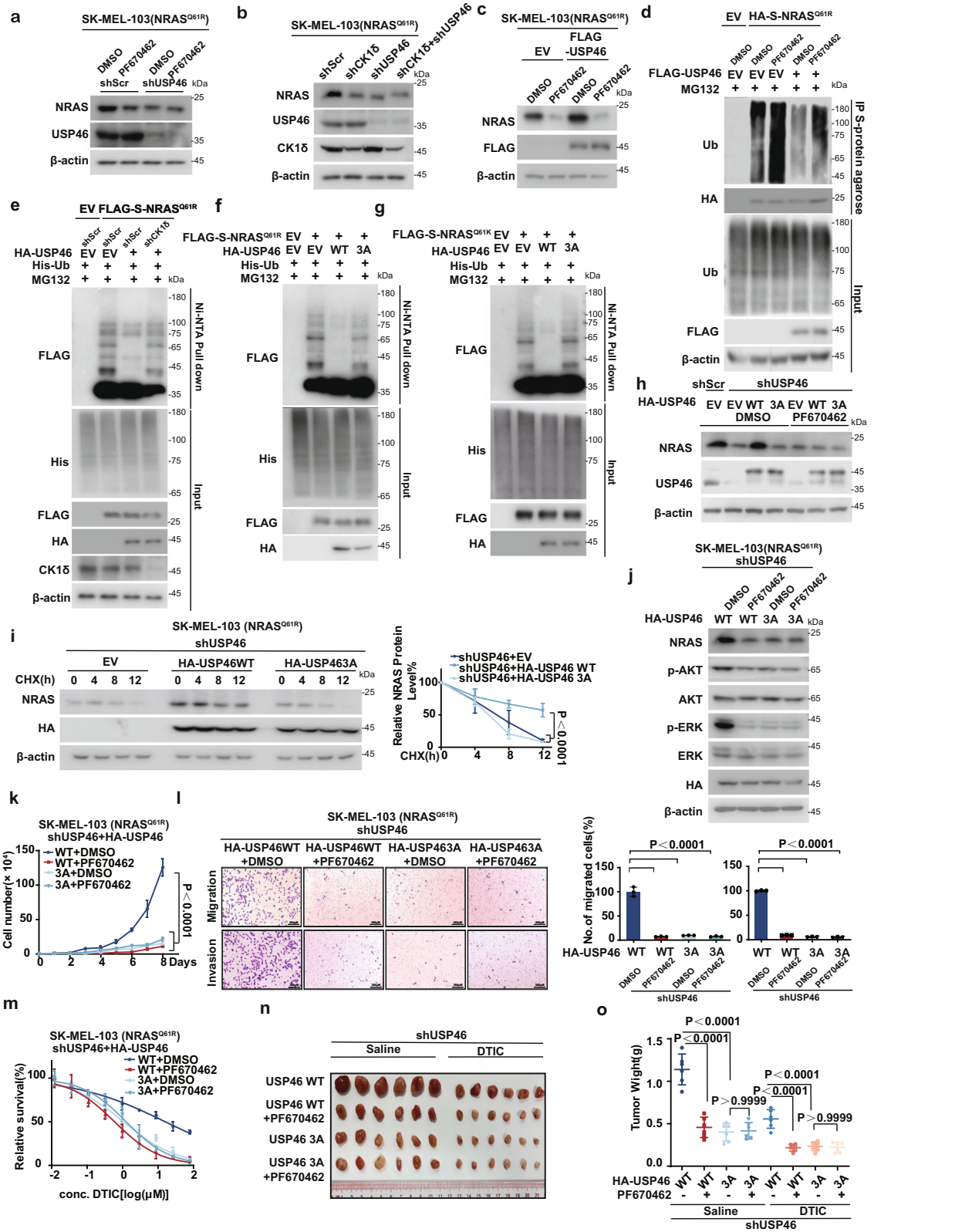

Considering these challenges, our findings identify a previously unknown oncogenic role of the CK1δ-USP46 axis by stabilizing NRAS Q61R/K mutants and provide important preclinical evidence that targeting the CK1δ-USP46 axis is an appealing strategy in the treatment of melanoma and other cancers with NRAS Q61R/K. However, melanoma is one of the most heterogeneous human cancers and displays a high level of genetic, molecular, and phenotypic diversity during tumor progression, thereby contributing to distinct treatment response and resistance. Thus, the heterogeneity in melanoma harboring NRAS Q61R/K mutants should be investigated in the future by single-cell RNA sequencing and other technologies, which may help understand the mechanisms of treatment response and provide further insights to prevent or overcome drug resistance to the pharmacological inhibition of the CK1δ-USP46 axis.

Fig. 7 | CK1δ-mediated phosphorylation of USP46 regulates tumor progression of oncogenic NRAS-driven melanoma. a NRAS and USP46 levels in SK-MEL-103 cells expressing shScramble (shScr) or shUSP46 treated with DMSO or PF670462 (5 μM) was examined. **b** NRAS and USP46 levels in SK-MEL-103 cells expressing shScr, shUSP46 and shCK1δ were examined. **c** SK-MEL-103 cells expressing empty vector (pLV3) or FLAG-USP46 were treated with DMSO or PF670462 (5 μM) and NRAS levels were examined. **d** Cells were transfected as indicated and treated with DMSO or PF670462 (5 μM) followed by MG132 treatment. Polyubiquitylated NRAS Q61R was examined. **e** Cells were cotransfected with empty vector, pIRES-NRAS Q61R and other plasmids. His-tagged ubiquitin was pulled-down by Ni-NTA beads and polyubiquitylated NRAS Q61R was examined. SK-MEL-103 and SK-MEL-30 cells were cotransfected with empty vector, pIRES-NRAS Q61R (**f**), pIRES-NRAS Q61K (**g**) and other indicated plasmids. His-tagged ubiquitin was pulled-down by Ni-NTA beads and polyubiquitylated NRAS Q61R/K was examined. **h** SK-MEL-103 cells stably expressing shScr or shUSP46 were transfected with empty vector (pLV5), USP46 WT or the 3A mutant. Cells were treated with DMSO or PF670462 and western blotting was performed. **i** SK-MEL-103 cells expressing shUSP46 were transfected with empty vector, USP46 WT or the 3A mutant and cycloheximide pulse-chase assay was performed. **j** SK-MEL-103 cells with endogenous USP46-deficiency were transfected with indicated plasmids and western blotting was performed. Proliferation (**k**), migration and invasion abilities (**l**) of cells (**j**) were examined and quantified. **m** SK-MEL-103 cells (**j**) were treated with DMSO or PF670462 (5 μM) and sensitivity to dacarbazine (DTIC) was determined. **n**, **o** SK-MEL-103 cells (**j**) were subcutaneously implanted into nude mice (5–6 weeks, $n = 6$). When tumors reached around 150–200 mm^3 in size, mice were treated with saline, PF670462 (4 mg/kg), DTIC (8 mg/kg) or PF670462 plus DTIC. Tumors were collected (**n**) and weights were measured (**o**). The results represent the mean ± s.d. of data from six mice. Immunoblots are representative of three independent experiments (**i**, **j**). Data were presented as mean ± SD of three independent experiments (**k**–**m**). Data were analyzed by two-sided one-way ANOVA in (**i**, **k**, **l**, **o**). Source data are provided as a Source Data file.

Methods

Ethical statement

This research complies with all relevant ethical regulations. All animal experiments were conducted in accordance with the protocols approved by the Institutional Animal Care and Use Committee of the Jinan University. The experiment using patients' samples was approved by the institutional ethics committee of Peking University Cancer Hospital and Research Institute.

Cell culture, plasmids and antibodies

HEK293T, A375, A2058, SK-MEL-2, SK-MEL-5, SK-MEL-28, HCT116, LoVo, AsPC-1, SU.86.86, A549, NCI-H358 cells and other lines were obtained from ATCC (American Type Culture Collection). HEK293T, A375, A2058, SK-MEL-2, SK-MEL-5 and SK-MEL-28 cells cultured in Dulbecco's modified Eagles's medium (Gibco) supplemented with 10% FBS (Gibco) or in Eagle's Minimum Essential medium (Gibco) supplemented with 10% FBS. HCT116 cells were cultured in McCoy's 5A medium (Gibco) with 10% FBS. A549, LoVo cells were cultured in F-12K medium (Gibco) with 10% FBS. NCI-H358, SU.86.86 and AsPC-1 cells were cultured in RPMI 1640 medium (Gibco) with 10% FBS. SK-MEL-103 was kindly shared by Dr. Jun Wan in Shenzhen PKU-HKUST Medical Centre. SK-MEL-30 was provided by the Cell Bank, Chinese Academy of Sciences. Immortal human melanocytes (hTERT/$CDK4^{R24C}$/$p53^{DD}$) were cultured in glutamine containing Ham's F12 media supplemented with 7% fetal bovine serum (FBS), 0.1 mM IBMX, 50 ng/mL TPA, 1 μM Na_3VO_4, and 1 μM dibutyryl cAMP. All cell lines were mycoplasma-free and authenticated by short tandem repeat DNA profiling analysis.

USP46 (NM_022832.4), CK1δ (NM_139062.4) and NRAS WT (NM_002524.5), and were cloned into pIRES-FLAG-S, pLV3-FLAG-S, pLV3-FLAG, pLV5-HA-S, pLVX3-GST, PET28A and pGEX4T-1 vectors, respectively. All site mutants of NRAS, KRAS and HRAS were generated by site-directed mutagenesis and identified by sequencing. In shRNA experiments, pLKO.1–scramble shRNA was used as a negative control with the sequence of CCTAAGGTTAAGTCGCCCTCG. The shRNA targeting sequences for USP46 shRNA#1 and shRNA#2 are 5′ - TCCA TGAAACTTACGCAGTAA −3′ and 5′ - CGCTTACCAATGAAACTCGAT −3′. The sequences for CK1δ shRNA#1 and shRNA#2 are 5′- CCACGTG AACTCGGTTGTAAC −3′ and 5′-CTCTGTTACCAATGGCTTTAC-3′. The sequence for CK1ε shRNA#1 is 5′- GCTTAGTGTCTTCACTGTATT −3′ and shRNA#2 is 5′-CCAGTGTTTGCTTAGTGTCTT-3′. For the overexpression experiments, the empty vectors were used as a negative control. The list of primers used in this study is in Supplementary Data.

Antibodies anti-p-AKT (Ser473) antibody (#4060S, dilution: 1:1000) and anti-AKT (pan) antibody (#2920S, dilution: 1:1000), phospho-p44/42 MAPK (Thr202/Tyr204) (#9101S, dilution: 1:1000) and p44/42 MAPK (ERK1/2) (#9102S, dilution: 1:1000), anti-β-catenin antibody (#9562S, dilution: 1:1000), LaminB (#13435S, dilution: 1:2000) and GAPDH (#5174S, dilution: 1:2000), anti-EGFR antibody (#4267S, dilution: 1:1000), anti-phospho-EGFR (Tyr1068) antibody (#3777S, dilution: 1:1000), anti-p38 MAPK (#9212S, dilution: 1:1000), anti-phospho-p38 MAPK (Thr180/Tyr182) (#9211S, dilution: 1:1000), cleaved caspase-3 antibody (#9664S, dilution: 1:200 for IHC) were purchased from CST (Cell Signaling Technology). Antibodies anti-CK1δ (14388-1-AP, dilution: 1:500) and anti-USP46 (13502-1-AP, dilution: 1:500) were purchased from Proteintech Group. Anti-NRAS (sc-31, dilution: 1:200), anti-p-Ser (sc-81514, dilution: 1:500), anti-p-Thr (H-2) (sc-5267, dilution: 1:500) and anti-Ub (sc-8017, dilution: 1:1000) antibodies were purchased from Santa Cruz Biotechnology. Light or heavy chain specific IPKine™ HRP (A25022 and A25112) were purchased from Abbkine Scientific Co were used in co-IP experiment. Anti-Ki67 antibody (SR00-02; dilution: 1:200 for IHC) was purchased from HUABIO. Anti-FLAG (F1804, dilution: 1:1000), anti-HA (H3663, dilution: 1:1000), anti-β-actin (A1978, dilution: 1:5000) and monoclonal anti-FLAG® M2-Peroxidase (HRP) (A8592, dilution: 1:1000) antibodies were purchased from Sigma-Aldrich. Antibodies anti-His tag (ab9108, dilution: 1:1000), anti-GST (ab111947, dilution: 1:1000) and anti-MYC tag (ab32, dilution: 1:1000) were purchased from Abcam.

siRNA transfection assay

For siRNA transfection, cells were transfected twice at 24 h intervals with control siRNA or target-specific siRNA using Oligofectamine (Invitrogen) following the manufacturer's instructions. After 24 hours of transfection, cells were subjected to the indicated treatment, and indicated protein expression levels were measured by western blotting. The siRNAs were synthesized by GenePharma (Shanghai, China). The sequences used were as follows: NC siRNA sense strand, 5′-UUCUCCGAACGUGUCACGUTT-3′ and antisense strand, 5′-ACGUGAC ACGUUCGGAGAATT-3′; β-catenin siRNA#1 sense strand, 5′-GCUGC UUUAUUCUCCCAUUTT-3′ and antisense strand, 5′-AAUGGGAGAA UAAAGCAGCTT-3′; β-catenin siRNA#2 sense strand, 5′- GGACACAG CAGCAAUUUGUTT-3′ and antisense strand, 5′- ACAAAUUGCUGCUG UGUCCTT-3′.

Small molecule compound screening by RAS GTPase ELISA assay

The small molecule compounds library from College of Pharmacy, Jinan University contains 1600 compounds supplied in 96-well plates. SK-MEL-103 cells stably expressing FLAG-NRAS Q61R were treated with DMSO or each compound from the library at the concentration of 10 μM for 24 hours. Cell lysates were then collected and NRAS activity was examined by modified RAS GTPase ELISA. 50 μL purified GST-RBD protein at the concentration of 2 μg/mL was added into each well of GSH-coated plate (Corning, CLS-9018) and incubated for 1 hour at room temperature with mild agitation. The plate was washed by cold PBS for three times. Cell lysate was then added to each well and incubated at 4 °C overnight followed with three times of washing by

https://doi.org/10.1038/s41467-024-54140-1

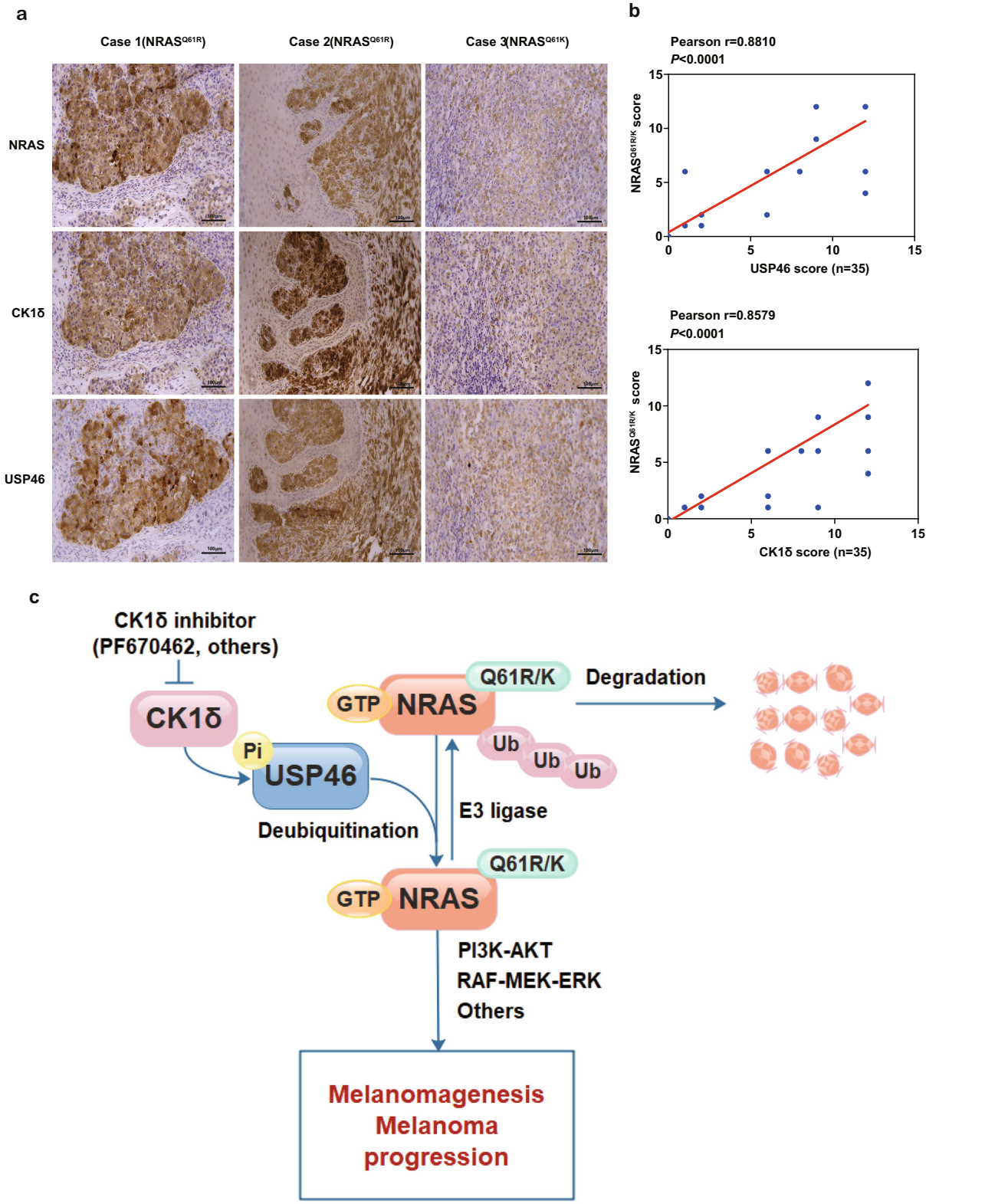

Fig. 8 | The expression of NRAS Q61R/K mutants positively correlates with USP46 and CK1δ in melanoma. a Representative images of immunohistochemical staining of USP46, CK1δ and NRAS in tumor samples of melanoma harboring NRAS Q61R ($n = 19$) or NRAS Q61K ($n = 16$). **b** Correlation of NRAS Q61R/K expression with USP46 and CK1δ was analyzed, respectively. Significant correlations were determined using a two-tailed Pearson correlation ($n = 35$). **c** This working model to illustrate that CK1δ phosphorylation-dependent activation of USP46 regulates tumorigenesis proliferation, migration, invasion and chemoresistance through stabilizing NRAS Q61R/K mutant.

PBS. The bound active FLAG-NRAS Q61R was then incubated with anti-FLAG antibody conjugated to HRP at room temperature for 60 min. The 3,3',5,5'-Tetramethylbenzidine (Aladdin, Shanghai, China) was added to generate a sensitive chemiluminescence readout at the wavelength of 450 nm. The levels of RBD-bound FLAG-NRAS Q61R after the treatment of each compound were quantified in relation to vehicle.

Western blotting analysis

Cells were lysed in NETN buffer [pH 8.0, 300 mM NaCl, 20 mM Tris-HCl, 0.5% NP-40, 1 mM ethylenediaminetetraacetic acid (EDTA)] containing protease inhibitors (1× protease inhibitor cocktail, 1 mM sodium orthovanadate, 10 mM β-glycerophosphate, 1 mM phenylmethylsulfonyl fluoride, and 10 mM sodium fluoride). Proteins were separated by SDS-PAGE gel electrophoresis and transferred to PVDF membranes, then incubated with the indicated primary and secondary antibodies.

Tandem affinity purification and mass spectrometry analyses

In brief, tandem affinity purification in cells expressing FLAG-S empty vector, FLAG-S-NRAS Q61R or FLAG-S-USP46 was conducted by combining FLAG-tag purification with anti-FLAG affinity gel (first purification) followed by the immunoprecipitation with the S-protein agarose (second purification). SK-MEL-103 cells were transfected with FLAG-S-tagged empty vector, FLAG-S-NRAS Q61R or FLAG-S-USP46. Cells were treated with MG132 (10 μM) for 10 hours and cell pellets were then collected and lysed in NETN buffer (pH 8.0, 300 mM NaCl, 20 mM Tris-HCl, 0.5% NP-40, 1 mM ethylenediaminetetraacetic acid (EDTA)) containing protease inhibitors (1×protease inhibitor cocktail (Roche), 1 mM sodium orthovanadate, 10 mM β-glycerophosphate, 1 mM phenylmethylsulfonyl fluoride, and 10 mM sodium fluoride). 20 μL Anti-FLAG Affinity Gel (Sigma-Aldrich) was added into cell lysates and rotated at 4 °C for 2 h. Anti-FLAG immunoprecipitates were washed three times with cold NETN buffer and incubated with 100 μL 3×FLAG peptide working solution at the concentration of 100 ug/mL (Sigma-Aldrich, F4799) at 4 °C for 2 h. The elution process was repeated for three additional times and the combination of elutes were diluted by NETN buffer. For the second purification step, 50 μL S-protein agarose (Merck Millipore) were added into the diluted elutes and incubated at 4 °C for 4 h. The immunoprecipitates by S-protein agarose were washed by NETN buffer for three times. The beads were resuspended in 500 μL 6 M urea in PBS, 25 μL of 200 mM DTT in 25 mM NH_4HCO_3 buffer was added and the reaction was incubated for 37°C for 30 min. For alkylation, 25 μL of 400 mM IAA in 25 mM NH_4HCO_3 buffer was added followed by incubation for 30 min at room temperature in dark. The supernatant was then removed and the beads were washed with 1 mL PBS once. For the digestion, 150 μL 2 M urea in PBS, 150 μL 1 mM $CaCl_2$ in 50 mM NH_4HCO_3 and 1 μL of trypsin (1.0 μg/μL) were added. The reaction was incubated at 37°C overnight. After evaporation in speedvac, the samples were tested by LC-MS/MS, equipped with an EASY-nLC 1200 HPLC system and QE Plus mass spectrometer (Thermo Fisher Scientific). About 1 μg of each sample was injected into a trap column (75 μm × 2 cm, C18, 3 μm, 100 Å, 164535) and an AcclaimPepMapC18 RSLC 75 μm ID × 25 cm separation column in an EASY-Spray setting, three injections were loaded for each sample continuously. Peptides were separated with a 70-min gradient (buffer A: 0.1% formic acid in deionized water; buffer B: 0.1% formic acid in 80% acetonitrile with a flow rate of 0.3 μL/min: 51 min of 4-28% B, 5 min of 28-38% B, 4 min of 38-90% B, 5 min of 90-4%B, 5 min of 4%B). Separated peptides were then directly analyzed on the QE Plus in a data-dependent manner. Peptides were ionized by using spray voltage of 2.4 kV and the ion transfer tube temperature was 320 °C, with automatic switching between MS and MS/MS scans using exclusion duration 25 s. Mass spectra were acquired at a resolution of 60,000 with a target value of 3×10^6 ions or a maximum integration time of 20 ms. The scan range was limited from 350 to 1500 m/z. Peptide S44 fragmentation was performed via higher-energy collision dissociation (HCD) with the energy set to 30%. High-resolution MS2 spectra were acquired with an exclusion duration of 25 s in the QE Plus with a maximum injection time of 40 ms at 17500resolution (isolation window 1.6 m/z), an AGC target value of 1×10^5 and normalized collision energy of 30%. The fixed first m/z was 100, and the isolation window was 1.6 m/z[55]. The raw data were processed by using Proteome Discoverer 2.5 and processed as per default workflow. MS tolerance is 4.5 ppm, and MS/MS tolerance is 20 ppm. Searches were performed against the Homo sapiens uniport canonical 20395 entries 20210516 nm fasta. Reversed database searches were used to evaluate false discovery rate (FDR) of site, peptide and protein identifications. Two missed cleavage sites of trypsin were allowed. Three independent LC-MS/MS of FLAG-S-NRAS Q61R and empty vector were analyzed based on abundances and protein hits were refined by corresponding volcano plots as (Log_2 fold change ratio of FLAG-S-NRAS Q61R/empty vector) against statistical significance ($-Log_{10}$ p value). Protein hits with Log_2 of fold change of NRAS Q61R/empty vector larger than 2 and $-Log_{10}$ p value larger than 1.35 in mass spectrum experiments were further considered.

Colony formation assay

The colony formation and in vivo tumorigenesis assay with the immortalized hTERT/CDK4^{R24C}/p53^{DD}/NRAS (Q61R) melanocytes were performed to investigate the melanocyte transformation[56,57]. For the colony formation assay, the hTERT/CDK4^{R24C}/p53^{DD}/NRAS (Q61R) melanocytes infected with indicated plasmids were plated into 6-well plate at 2,500 cells per well and cultured for 14 days. The colonies were fixed with 10% (v/v) methanol for 15 min and stained with 5% Giemsa (Sigma) for 30 min for colony visualization. Colonies were imaged and quantified using Image J. Images were converted to an 8-bit grayscale format, thresholded to highlight the colonies, and converted to a binary image (black colonies on white background). The 'Analyze Particles' function was used to count number of colonies.

In vitro kinase assay

Cell lysates of SK-MEL-103 cells stably expressing FLAG-CK1δ were immunoprecipitated with anti-FLAG affinity gel. GST, GST-USP46 WT, the single mutants and the 3 A mutant protein was purified from SK-MEL-103 cells stably expressing empty vector, pLVX3-GST-USP46 WT and mutants using Pierce Glutathione agarose. The proteins were then eluted with washing buffer (10 mM GSH and 50 mM Tris-HCl, pH 8.0) and purified with Ultrafiltration tube. Immunoprecipitated CK1δ was incubated with 1 μg of purified GST, GST-USP46 WT and indicated mutants in the kinase buffer (50 mM Tris-HCl pH 7.4, 10 mM $MgCl_2$, 0.02% bovine serum albumin, 1 mM DTT, 0.1 mM ATP). The reaction was carried out in the presence of DMSO or PF670462 (5 μM) at 30 °C for 60 min and stopped by the addition of SDS loading buffer. Then analyzed by western blotting.

Phos-tag SDS-PAGE

In brief, SuperSep™ Phos-tag™ (50 μM), 7.5%, 17well, 83×100×3.9 mm are commercially available from FUJIFILM Wako Pure Chemical Corp. (Osaka, Japan). The running buffer consisted of Tris-base (0.25 M), 0.10% w/v SDS, glycine (1.92 M). Electrophoresis was performed at 30 mA/gel until the bromophenol blue dye reached the bottom of the separating gel. After electrophoresis, the gel was shaked gently in transfer buffer containing 10 mM EDTA and transferred to PVDF membranes (Merck Millipore). Western blotting was subsequently performed with indicated antibodies.

Immunoprecipitation

Cells transfected with indicated plasmids were lysed in NETN buffer and were incubated 2 hours with anti-FLAG affinity gel or S-protein agarose for 4 hours at 4 °C. SK-MEL-103, SK-MEL-30 or SK-MEL-2 cells

as indicated were lysed in NETN buffer and were incubated overnight with primary antibodies together with protein A/G beads at 4°C. The immunoprecipitates were washed for three times and subjected to western blotting.

Denaturing immunoprecipitation for ubiquitination and denaturating Ni-NTA pulldown. The cells were lysed in 100 ml 62.5 mM Tris-HCl (pH 6.8), 10% glycerol, 2% SDS, 1 mM iodoacetamide and 20 mM NEM, boiled for 15 min, diluted 10 times with NETN buffer containing protease inhibitors, 20 mM NEM and 1 mM iodoacetamide, then centrifuged to remove cell debris. Cell extracts were subjected to immunoprecipitation with the indicated antibodies and blotted as indicated antibody. Denaturating Ni-NTA pulldown was performed as previously described[58].

Glutathione-S-transferase (GST) pull-down assay

Recombinant GST-CK1δ or GST-USP46 and His-KRAS WT, His-HRAS WT, His-NRAS WT or His-KRAS MUT, His-HRAS MUT, His-NRAS Q61MUT proteins were expressed in Escherichia coli strain BL21. GST, GST-CK1δ or GST-USP46 protein was purified using Pierce Glutathione agarose. Fusion proteins were mixed for 4 hours at 4 °C. Beads were washed four times, and proteins were detected by western blotting.

In vitro ubiquitination assay

Cells transfected with HA-S-NRAS Q61R were treated with 10 mM MG132 for 10 hours. NRAS Q61R was pull-downed by S-protein agaroses, which was detected with an anti-HA antibody. The recombinant GST-fused USP46 WT and C44S mutant protein was expressed in Escherichia coli strain BL21 and purified using Pierce Glutathione Agarose. The proteins were then eluted with GST elution buffer (10 mM GSH and 50 mM Tris-HCl, pH 8.0). The ubiquitinated NRAS Q61R protein was then incubated with purified GST-USP46 WT and C44S protein separately for 4 hours at 4°C, followed by western blotting analysis.

Quantitative real-time PCR (qRT-PCR)

RNA extraction from cultured cells was performed using TRIzol reagent (Thermo Scientific, MA, USA), and then RNA was subsequently reverse transcribed to cDNA using a FastKing gDNA Dispelling RT SuperMix (Tiangen, Beijing, China). qRT-PCR analysis was performed using FastFire qPCR PreMix (SYBR Green). All experiments were performed in triplicate with three commonly used housekeeping genes *GADPH, 18s* and *β-actin* as the internal control. Primer sequences are listed. *NRAS* Forward 5′- GCAAGTCATTTGCGGATATTAAC-3′, Reverse 5′-CATCCGAGTCTTTTACTCGCTTA-3′. *CK1δ* Forward 5′-ACAACGTC ATGGTGATGGAG-3′, Reverse 5′-GAATGTATTCGATGCGACTGAT-3′. *CK1ε* Forward 5′-TGAGTATGAGGCTGCACAGG −3′, Reverse 5′-TCAAA TGGCACACTTGTCTGT −3′. *GAPDH* Forward 5′-GATCGAATTAAACCTT ATCGTCGT −3′, Reverse 5′-GCAGCAGAACTTCCACTCGGT −3′. *18s* Forward 5′-GAGGATGAGGTGGAACGTGT-3′, Reverse 5′-AGAAGTGAC GCAGCCCTCTA-3′. *β-actin* Forward 5′-GCACCACACCTTCTACAATG −3′, Reverse 5′-TGCTTG CTGATCCACATCTG-3′.

Cell proliferation assay

SK-MEL-103, SK-MEL-30 or SK-MEL-2 cells (4×10^4) were seeded in each well. Cells from each well were digested with 0.25% trypsin at 37°C the next day. And cell pellets were collected by centrifugation, washed by PBS, re-suspended in PBS and counted under microscope. Likewise, cells for the next 8 days were counted in similarly method.

Migration and invasion assay

For migration assays, cells were seeded in 24-well Cell Culture Insert (BD, 353097). For invasion assays, cells were seeded in 24-well Cell Culture Insert (BD, 353097) with matrigel. After 48 hours, the filter was fixed with 4% Para-formaldehyde and stained with 0.5 % crystal violet, and then migrating and invading cells were counted.

CCK-8 assay

A Cell Counting Kit-8 (HY-K0301) was used to measure the survival of SK-MEL-103, SK-MEL-30 or SK-MEL-2 cells. A total of 2000 cells in a volume of 100 µL per well were cultured in three replicate wells in a 96-well plate in medium containing 10% FBS. Cells were treated with vehicle, PF670462 (5 µM) or different concentrations of DTIC for 72 hours and CCK-8 reagent (15 µL) was added and incubated for 2 hours.

Animal studies

All animal experiments were performed in accordance with a protocol approved by the Institutional Animal Care and Use Committee of the Jinan University (20220419-04). 5-6-weeks-old BALB/c female nude mice were obtained from Jicui Yaokang Biotechnology Co., Ltd. of China, and were randomly allocated to experimental groups. All animals were housed at a suitable temperature (22-24 °C) and humidity (40-70%) under a 12/12-h light/dark cycle with unrestricted access to food and water for the duration of the experiment. The xenograft experiment follows the humane endpoint. Indicators such as huddled posture, immobility, ruffled fur, failure to eat, hypothermia (colonic temperature of <34 °C), or weight loss (> 20%) may be useful objective criteria for early euthanasia. The animals will be euthanized immediately if they are unable to stand or if they display agonal breathing, severe muscular atrophy, severe ulceration, or uncontrolled bleeding. The subcutaneous tumor maximum volume was 2000 mm^3 and authorized by the Committees on Animal Research and Ethics, and was not exceeded at any time during the experiments. For subcutaneous xenografting, hTERT/$CDK4^{R24C}$/$p53^{DD}$ human melanocytes (2×10^6) or SK-MEL-103 cells (2×10^6) infected with indicated plasmids were mixed with Matrigel (1:1) and subcutaneously implanted into the flanks of female BALB/c nude mice (n = 6). The tumor volumes were measured three times weekly by using a Vernier caliper to measure the short diameter and long diameter of the tumor. Tumor volumes were calculated using the following formula: $width^2 \times length \times 0.4$ (mm^3). When tumors reached 150-200 mm^3 in size, mice were administered saline or PF670462 (4 mg/kg) every 3 days. DTIC (8 mg/kg) was administered three times per week. After the tumors had grown for the designated time, all mice were euthanized, and the tumors were harvested.

Immunohistochemical staining

Tissue sections of *NRAS Q61MUT* melanoma were obtained from the tissue bank at the Peking University Cancer Hospital and Research Institute in accordance with the approval document of the Institutional Medical Ethics Committee (2016KT59). Anti-NRAS (sc-31, dilution: 1:100) and anti-CK1δ (14388-1-AP, dilution: 1:200), anti-USP46 (13502-1-AP, dilution: 1:200) antibodies was used for immunohistochemical staining of formalin-fixed paraffin-embedded of melanoma tissues were incubated out at 4°C for 12 hours. The immunostaining was randomly scored by two pathologists. The IHC score was calculated by combining the quantity score (percentage of positive stained tissues) with the staining intensity score. The score for each tissue was calculated by multiplying the quantity with the intensity score (the range of this calculation was therefore 0-12). An IHC score of 9-12 was considered a strong immunoreactivity; 5-8, moderate; 1-4, weak; and 0, negative. Samples with IHC score > 4 were considered to be high, and ≤ 4 were considered to be low. The Pearson correlation was used f or statistical analysis of the correlation between CK1δ, USP46 and NRAS mutants.

In tumors from animal experiments, H&E and immunostaining of Ki67 and cleaved caspase-3 were performed. In brief, tumors samples were fixed with 4% paraformaldehyde, embedded in paraffin, and microtome sliced into 5 µm sections. Following dewaxing and dehydrating, anti-Ki67 (dilution: 1:200) and cleaved caspase-3 (dilution: 1:200) antibodies were used for immunohistochemical

staining of tumor sections from mice. H&E staining of the slides was performed according to the manufacturer's instructions (E607318; Sangon Biotech). Slices were then imaged using a microscope (Olympus).

Statistics and reproducibility

Cell proliferation, migration, invasion, and survival experiments was independently performed for three times, following the principle of repeatability. In the animal study, data represent as the mean ± s.d. of six mice. Statistical analyses were performed using GraphPad Prism software version 9.3. One-way ANOVA analysis and Tukey's test or *t*-test was used to compare results.

Reporting summary

Further information on research design is available in the Nature Portfolio Reporting Summary linked to this article.

Data availability

All data generated or analyzed during this study are included within the article, Supplementary Information, the Source Data file, and the protein mass spectrometry raw data are available through the ProteomeXchange Consortium (http://www.proteomexchange.org/) via the PRIDE partner repository with dataset identifiers PXD046277 and PXD051431. Source data are provided with this paper.

References

1. Pylayeva-Gupta, Y., Grabocka, E. & Bar-Sagi, D. RAS oncogenes: weaving a tumorigenic web. *Nat. Rev. Cancer* **11**, 761–774 (2011).
2. Chen, K., Zhang, Y., Qian, L. & Wang, P. Emerging strategies to target RAS signaling in human cancer therapy. *J. Hematol. Oncol.* **14**, 116 (2021).
3. Jakob, J. A. et al. NRAS mutation status is an independent prognostic factor in metastatic melanoma. *Cancer* **118**, 4014–4023 (2012).
4. Murphy, B. M. et al. Enhanced BRAF engagement by NRAS mutants capable of promoting melanoma initiation. *Nat. Commun.* **13**, 3153 (2022).
5. Skoulidis, F. et al. Sotorasib for lung cancers with KRAS p.G12C mutation. *N. Engl. J. Med.* **384**, 2371–2381 (2021).
6. Zhang, Z., Guiley, K. Z. & Shokat, K. M. Chemical acylation of an acquired serine suppresses oncogenic signaling of K-Ras(G12S). *Nat. Chem. Biol.* **18**, 1177–1183 (2022).
7. Hallin, J. et al. Anti-tumor efficacy of a potent and selective non-covalent KRAS(G12D) inhibitor. *Nat. Med.* **28**, 2171–2182 (2022).
8. Narasimamurthy, R. et al. CK1δ/ε protein kinase primes the PER2 circadian phosphoswitch. *Proc. Natl Acad. Sci. USA* **115**, 5986–5991 (2018).
9. Kloss, B. et al. The Drosophila clock gene double-time encodes a protein closely related to human casein kinase Iepsilon. *Cell* **94**, 97–107 (1998).
10. Behrend, L. et al. IC261, a specific inhibitor of the protein kinases casein kinase 1-delta and -epsilon, triggers the mitotic checkpoint and induces p53-dependent postmitotic effects. *Oncogene* **19**, 5303–5313 (2000).
11. Wang, Z. et al. The CK1δ/ε-AES axis regulates tumorigenesis and metastasis in colorectal cancer. *Theranostics* **11**, 4421–4435 (2021).
12. Rosenberg, L. H. et al. Therapeutic targeting of casein kinase 1δ in breast cancer. *Sci. Transl. Med.* **7**, 318ra202 (2015).
13. Shin, S., Wolgamott, L., Roux, P. P. & Yoon, S. O. Casein kinase 1ε promotes cell proliferation by regulating mRNA translation. *Cancer Res.* **74**, 201–211 (2014).
14. Long, A., Zhao, H. & Huang, X. Structural basis for the interaction between casein kinase 1 delta and a potent and selective inhibitor. *J. Med. Chem.* **55**, 956–960 (2012).
15. Yin, C. et al. Pharmacological targeting of STK19 inhibits oncogenic NRAS-driven melanomagenesis. *Cell* **176**, 1113–1127.e1116 (2019).
16. Eggermont, A. M. M. & Kirkwood, J. M. Re-evaluating the role of dacarbazine in metastatic melanoma: what have we learned in 30 years? *Eur. J. Cancer* **40**, 1825–1836 (2004).
17. Sinnberg, T. et al. Suppression of casein kinase 1alpha in melanoma cells induces a switch in beta-catenin signaling to promote metastasis. *Cancer Res.* **70**, 6999–7009 (2010).
18. Sinnberg, T., Wang, J., Sauer, B. & Schittek, B. Casein kinase 1α has a non-redundant and dominant role within the CK1 family in melanoma progression. *BMC Cancer* **16**, 594 (2016).
19. Lee, S. K. et al. β-Catenin-RAS interaction serves as a molecular switch for RAS degradation via GSK3β. *EMBO Rep.* **19**, e46060 (2018).
20. Jeong, W. J., Ro, E. J. & Choi, K. Y. Interaction between Wnt/β-catenin and RAS-ERK pathways and an anti-cancer strategy via degradations of β-catenin and RAS by targeting the Wnt/β-catenin pathway. *NPJ Precis. Oncol.* **2**, 5 (2018).
21. Jeong, W. J. et al. Ras stabilization through aberrant activation of Wnt/β-catenin signaling promotes intestinal tumorigenesis. *Sci. Signal.* **5**, ra30 (2012).
22. Huang, L. Y. et al. SCF(FBW7)-mediated degradation of Brg1 suppresses gastric cancer metastasis. *Nat. Commun.* **9**, 3569 (2018).
23. Hu, Z. & Martí, J. Isomer-sourced structure iteration methods for in silico development of inhibitors: Inducing GTP-bound NRAS-Q61 oncogenic mutations to an "off-like" state. *Comput. Struct. Biotechnol. J.* **23**, 2418–2428 (2024).
24. Najm, P. et al. Loss-of-function mutations in TRAF7 and KLF4 cooperatively activate RAS-like GTPase signaling and promote meningioma development. *Cancer Res.* **81**, 4218–4229 (2021).
25. Sasaki, A. T. et al. Ubiquitination of K-Ras enhances activation and facilitates binding to select downstream effectors. *Sci. Signal.* **4**, ra13 (2011).
26. Fulcher, L. J. & Sapkota, G. P. Functions and regulation of the serine/threonine protein kinase CK1 family: moving beyond promiscuity. *Biochem. J.* **477**, 4603–4621 (2020).
27. Randic, T., Kozar, I., Margue, C., Utikal, J. & Kreis, S. NRAS mutant melanoma: towards better therapies. *Cancer Treat. Rev.* **99**, 102238 (2021).
28. Pozniak, J. et al. A TCF4-dependent gene regulatory network confers resistance to immunotherapy in melanoma. *Cell* **187**, 166–183.e125 (2024).
29. Cheng, Y., Zhang, G. & Li, G. Targeting MAPK pathway in melanoma therapy. *Cancer Metastasis Rev.* **32**, 567–584 (2013).
30. Garutti, M. et al. CDK4/6 inhibitors in melanoma: a comprehensive review. *Cells* **10**, 1334 (2021).
31. Marin-Bejar, O. et al. Evolutionary predictability of genetic versus nongenetic resistance to anticancer drugs in melanoma. *Cancer Cell* **39**, 1135–1149.e1138 (2021).
32. Li, S., Song, Y., Quach, C., Nemecio, D. & Liang, C. Revisiting the role of autophagy in melanoma. *Autophagy* **15**, 1843–1844 (2019).
33. Di Leo, L. & De Zio, D. AMBRA1 has an impact on melanoma development beyond autophagy. *Autophagy* **17**, 1802–1803 (2021).
34. Mullarky, E., Mattaini, K. R., Vander Heiden, M. G., Cantley, L. C. & Locasale, J. W. PHGDH amplification and altered glucose metabolism in human melanoma. *Pigment Cell Melanoma Res.* **24**, 1112–1115 (2011).
35. Punekar, S. R., Velcheti, V., Neel, B. G. & Wong, K. K. The current state of the art and future trends in RAS-targeted cancer therapies. *Nat. Rev. Clin. Oncol.* **19**, 637–655 (2022).
36. Appleton, K. M. et al. Inhibition of the myocardin-related transcription factor pathway increases efficacy of trametinib in NRAS-mutant melanoma cell lines. *Cancers* **13**, 2012 (2021).

37. Najem, A. et al. P53 and MITF/Bcl-2 identified as key pathways in the acquired resistance of NRAS-mutant melanoma to MEK inhibition. *Eur. J. Cancer* **83**, 154–165 (2017).
38. Kim, S. E. et al. H-Ras is degraded by Wnt/beta-catenin signaling via beta-TrCP-mediated polyubiquitylation. *J. Cell Sci.* **122**, 842–848 (2009).
39. Baietti, M. F. et al. OTUB1 triggers lung cancer development by inhibiting RAS monoubiquitination. *EMBO Mol. Med.* **8**, 288–303 (2016).
40. Cheong, J. K. et al. IC261 induces cell cycle arrest and apoptosis of human cancer cells via CK1δ/ε and Wnt/β-catenin independent inhibition of mitotic spindle formation. *Oncogene* **30**, 2558–2569 (2011).
41. Catarzi, D. et al. Casein kinase 1δ inhibitors as promising therapeutic agents for neurodegenerative disorders. *Curr. Med. Chem.* **29**, 4698–4737 (2022).
42. Schittek, B. & Sinnberg, T. Biological functions of casein kinase 1 isoforms and putative roles in tumorigenesis. *Mol. Cancer* **13**, 231 (2014).
43. Richards, J. et al. Inhibition of αENaC expression and ENaC activity following blockade of the circadian clock-regulatory kinases CK1δ/ε. *Am. J. Physiol. Ren. Physiol.* **303**, F918–F927 (2012).
44. Li, D. et al. Casein kinase 1 enables nucleus accumbens amphetamine-induced locomotion by regulating AMPA receptor phosphorylation. *J. Neurochem.* **118**, 237–247 (2011).
45. Mente, S. et al. Ligand-protein interactions of selective casein kinase 1δ inhibitors. *J. Med. Chem.* **56**, 6819–6828 (2013).
46. Zhang, H. et al. Upregulation of stress-induced protein kinase CK1 delta is associated with a poor prognosis for patients with hepatocellular carcinoma. *Genet. Test. Mol. Biomark.* **25**, 504–514 (2021).
47. Knippschild, U. et al. p53 is phosphorylated in vitro and in vivo by the delta and epsilon isoforms of casein kinase 1 and enhances the level of casein kinase 1 delta in response to topoisomerase-directed drugs. *Oncogene* **15**, 1727–1736 (1997).
48. Webster, M. R. et al. Paradoxical role for wild-type p53 in driving therapy resistance in melanoma. *Mol. Cell* **77**, 633–644.e635 (2020).
49. Pandya, P., Kublo, L. & Stewart-Ornstein, J. p53 promotes cytokine expression in melanoma to regulate drug resistance and migration. *Cells* **11**, 405 (2022).
50. Meng, Z. et al. Kinase activity of casein kinase 1 delta (CK1δ) is modulated by protein kinase C α (PKCα) by site-specific phosphorylation within the kinase domain of CK1δ. *Biochim. Biophys. Acta Proteins Proteom.* **1867**, 710–721 (2019).
51. Meng, Z. et al. CK1δ kinase activity is modulated by protein kinase C α (PKCα)-mediated site-specific phosphorylation. *Amino Acids* **48**, 1185–1197 (2016).
52. Bischof, J. et al. CK1δ kinase activity is modulated by Chk1-mediated phosphorylation. *PLoS ONE* **8**, e68803 (2013).
53. Joshi, S. K. et al. The AML microenvironment catalyzes a stepwise evolution to gilteritinib resistance. *Cancer Cell* **39**, 999–1014.e1018 (2021).
54. Bolouri, H. et al. The molecular landscape of pediatric acute myeloid leukemia reveals recurrent structural alterations and age-specific mutational interactions. *Nat. Med.* **24**, 103–112 (2018).
55. Ma, N. et al. 2H-azirine-based reagents for chemoselective bioconjugation at carboxyl residues inside live cells. *J. Am. Chem. Soc.* **142**, 6051–6059 (2020).
56. Garraway, L. A. et al. Integrative genomic analyses identify MITF as a lineage survival oncogene amplified in malignant melanoma. *Nature* **436**, 117–122 (2005).
57. Lissanu Deribe, Y. et al. Truncating PREX2 mutations activate its GEF activity and alter gene expression regulation in NRAS-mutant melanoma. *Proc. Natl Acad. Sci. USA* **113**, E1296–E1305 (2016).
58. Liu, T. et al. CDK4/6-dependent activation of DUB3 regulates cancer metastasis through SNAIL1. *Nat. Commun.* **8**, 13923 (2017).

Acknowledgements

This study was supported by the National Key Research and 1054Development Program (2023YFC2506404 L.S.), National Natural Science Foundation of China (82473109 T.L., 81603133 Y.Z., 32100579 C.Y., 82341011 C.Y., 82272676 L.S., 82404654 Y.W.), Guangdong Basic and Applied Basic Research Foundation (2024A1515013266 T.L., 2024B1515040007 T.L., 2022A1515012371 Y.Z., 2024A1515010450 Y.Z. and 2020A1515110857 C.Y.), Guangdong Major Project of Basic and Applied Basic Research (2023B0303000026 T.L.), Major Talent Program of Guangdong Provincial (2019QN01Y933 T.L.), the project of State Key Laboratory of Functions and Applications of Medicinal Plants, Guizhou Medicinal University (QJJ[2022]420 T.L.), Fundamental Research Funds for the Central Universities (21622102 T.L.), Medical Joint Fund of Jinan University (YXJC2022006 T.L.) and National Key R&D Program of China (2022YFA0912600 C.Y.), Guangzhou Basic Research Program Basic and Applied Basic Research Project (2023A04J0645 Y.Z.). Shenzhen Medical Research Fund (B2302018 C.Y.), Major Program (S201101004 C.Y.) and Open Fund (SZBL2021080601004 C.Y.) of Shenzhen Bay Laboratory. China Postdoctoral Science Foundation (2024M750581 Y.W.), the "San Jia Si Qing" fund of the Affiliated Guangdong Second Provincial General Hospital of Jinan University (2024C002 Q.Z.), Guangdong Provincial Second People's Hospital Ph.D./Postdoctoral Workstation Program (2023BSGZ009 Y.W.), Beijing Municipal Administration of Hospitals' Ascent Plan (DFL20220901 L.S.), Beijing Natural Science Foundation (7242021 L.S.). The authors would like to thank the Institute of Molecular and Medical Virology, Jinan University for providing us with necessary experimental support by supplying protein purification system, laser scanning confocal microscope, ultracentrifuge, and other equipment for this study. The model of the structure of ubiquitinated NRAS in complex with USP46 are kindly performed by Dr Yang Zhou (Jinan University).

Author contributions

T.L. conceived the study and designed experiments. Y.W. performed most experiments with assistance from X.Y., H.W., M.L., C.Z., L.H., X.M., R.W., S.L., H.J. and Q.G. X.L. and Z.L. provided small molecule compounds. L.S. provided tissue sections of NRAS-mutant melanoma. T.L., Y.W. and X.Y. wrote the manuscript with input from C.Y., Y.Z. and Q.Z. T.L., C.Y., L.S. and Q.Z. guided and supervised the study. All the authors commented on the manuscript.

Competing interests

The authors declare no competing interests.

Additional information

Supplementary information The online version contains supplementary material available at https://doi.org/10.1038/s41467-024-54140-1.

Correspondence and requests for materials should be addressed to Qiushi Zhang, Lu Si, Chengqian Yin or Tongzheng Liu.

Peer review information *Nature Communications* thanks Anna Sablina, Tobias Sinnberg and the other, anonymous, reviewer(s) for their contribution to the peer review of this work. A peer review file is available.